

Application of optical hydrogels in environmental sensing

Shuo Yang¹, Shruti Sarkar², Xing Xie², Dan Li¹, and Jianmin Chen¹

¹Fudan University

²Georgia Institute of Technology

February 1, 2023

Abstract

The ever-increasing complexity of environmental pollutants urgently warrants the development of new detection technologies. In this context, sensors based on the optical properties of hydrogels enabling fast and easy in situ detection are attracting increasing attention. Herein, the target recognition and sensing mechanisms of two main types of optical hydrogels (OHs) are reviewed and discussed: photonic crystal hydrogels (PCHs) and fluorescent hydrogels (FHs). For PCHs, the environmental stimulus response, target receptors, inverse opal structures, and molecular imprinting techniques related to PCHs are reviewed and summarized. Furthermore, the different types of fluorophores (i.e., compound probes, biomacromolecules, quantum dots, and luminescent microbes) of FHs are summarized. Finally, the data from 138 papers about different OHs are extracted for secondary statistical analysis. The detection performance and potential of various OH types in different environmental pollutant detection scenarios are evaluated, and compared them to those obtained using the standard detection method. Based on this analysis, some possible development directions are proposed, including the fusion of various OHs, introduction of more hydrogel technologies from the biomedical field to the environmental pollutant detection field, and development of multifunctional sensor arrays.

Article category: Review

Subcategory: Environmental Optical Sensing

Application of optical hydrogels in environmental sensing

Shuo Yang, Shruti Sarkar, Xing Xie, Dan Li*, Jianmin Chen.*

Dr. S. Y. Author 1, Prof. D. L. Author 4, Prof. J. M. C. Author 5

Shanghai Key Laboratory of Atmospheric Particle Pollution and Prevention (LAP3), Department of Environmental Science and Engineering, Fudan University, Shanghai 200438, China.

E-mail: lidanfudan@fudan.edu.cn

S. S. Author 2, Prof X. X Author 3

School of Civil and Environmental Engineering, Georgia Institute of Technology, Atlanta, Georgia 30332, USA.

E-mail: xing.xie@ce.gatech.edu

Keywords: optical hydrogel; environmental sensors; contamination detection; photonic crystal hydrogel; Fluorescent hydrogel

The ever-increasing complexity of environmental pollutants urgently warrants the development of new detection technologies. In this context, sensors based on the optical properties of hydrogels enabling fast and easy in situ detection are attracting increasing attention. Herein, the target recognition and sensing mechanisms

of two main types of optical hydrogels (OHs) are reviewed and discussed: photonic crystal hydrogels (PCHs) and fluorescent hydrogels (FHs). For PCHs, the environmental stimulus response, target receptors, inverse opal structures, and molecular imprinting techniques related to PCHs are reviewed and summarized. Furthermore, the different types of fluorophores (i.e., compound probes, biomacromolecules, quantum dots, and luminescent microbes) of FHs are summarized. Finally, the data from 138 papers about different OHs are extracted for secondary statistical analysis. The detection performance and potential of various OH types in different environmental pollutant detection scenarios are evaluated, and compared them to those obtained using the standard detection method. Based on this analysis, some possible development directions are proposed, including the fusion of various OHs, introduction of more hydrogel technologies from the biomedical field to the environmental pollutant detection field, and development of multifunctional sensor arrays.

1. Introduction

Detecting and monitoring environmental pollutants are critical for modern disease prevention. Generally, pollutant detection relies on the chemical or microbial analysis of environmental samples using techniques and devices such as chromatography and mass spectrometry^[1], spectral analysis^[2], microbial sensors^[3], and immunoassays^[4]. Existing detection technologies have many limitations, including complex pretreatment, cost, and rigorous testing environments. Recently, the development of detection technologies has received contributions from different disciplines. Many novel materials, including functional nucleic acids, nanoparticles, graphene, metal-organic frameworks, and hydrogels^[5-9], have been applied for environmental sensing. Combining multiple technologies has become more common. Application and development of hydrogels are among the most noteworthy advancements in this field.

Hydrogels are soft and elastic molecular networks with high water content formed by the physical or chemical crosslinking of hydrophilic polymers^[10]. They have excellent porous structures, good biocompatibility, high responsiveness to environmental stimuli, and controllable physical (strength, toughness, swelling, viscosity, and specific surface area) and chemical properties. Ever since hydrogels were first synthesized and used in biomedicine in 1960^[11], their application fields have included optics, drug-loading and targeted therapy, cell culture, three-dimensional (3D) printing, bioembedding, tissue repair, robotics, and biodetection^[12-19]. Owing to their complex structures and chemical properties, most hydrogels can be chemically modified or grafted with different functional groups to obtain new properties^[20]. Interpenetrating polymeric or semi-interpenetrating polymer networks are formed by at least two different hydrogel molecular chains interpenetrating or semi-interpenetrating each other. Combining the properties of each comonomer can generate new properties^[21]. The most significant advantage of hydrogels is their compatibility with various materials, which allows them to effectively load nanomaterials, polymers, drugs, biomacromolecules, and even living cells^[22-25]. Moreover, as loading matrixes, hydrogels can retain and enhance the properties of their loaded contents and even eliminate some of their inherent defects. Therefore, hydrogels are ideal for many research fields, including environmental pollutant detection.

Nowadays, hydrogel-based materials are gaining popularity in the detection field, particularly for developing new sensors. Functionalized hydrogels coordinated with sensor elements, such as light sensors, pressure-sensing elements, thermosensitive elements, field-effect elements, enzymes, antibodies, and microorganisms, have been used to detect various analytes in biology and medicine^[26]. Notably, some hydrogels have good transparency and optical properties and have thus been widely used as new contact lens materials and replacements for cornea and crystalline lenses^[27,28]. Indeed, optical imaging and optical signal expression can benefit from most of the advantages of hydrogel sensors. Optical hydrogel (OH)-based sensors without specialized and complex analytical equipment enable the rapid detection of pollutants with simple equipment or even visual observation^[29]. Based on the statistical analysis of >1000 papers from the Web of Science Core Collection and their references, OH-related detection technologies have attracted increasing attention in recent years (**Figure 1**). In the past two years, researchers have developed several hydrogel-based detection systems with excellent performance, such as multifunctional detection sensors, selective sensors, and high-precision sensors. Environmental researchers have seen the potential of OHs and applied them to pollutant detection^[6,30], particularly for the fast and inexpensive in situ detection of environmental pollutants. How-

ever, OH sensor application studies primarily concentrate on biological and medical testing^[31,32]. Therefore, there is currently a lack of reviews and perspective studies on the applications of OHs in environmental sensing, particularly on the feasibility and design strategies for implementing OHs in the practical detection of environmental pollutants.

Herein, Sections 2 and 3 respectively review photonic crystal hydrogels (PCHs) and fluorescent hydrogels (FHs), two main types of OHs. They also detail the types of target pollutants that they can detect and their sensing mechanisms. Given the complex relationship between pathogenic microorganisms and contaminants, we also discuss some OHs for microbial detection. Next, Section 4 briefly reviews other types of OHs used for environmental sensing. Because OH research is far less active in environmental sensing than in the medical field, it is unclear how to determine the types of OHs that are most suitable when targeting specific pollutants. To address this, we performed a secondary statistical analysis of data extracted from 138 papers (**Section 5**). Section 5 discusses the types of pollutants that could be detected by different OHs, the detection sensitivity, the relationship between different OHs, and the application potential of various types of OHs in the field of pollutant detection. Based on this analysis, we then propose some future research directions for intelligent, high-sensitivity, and rapid OH-based pollutant detection technologies. Table 1 lists all the abbreviations used in this review. Table 2 lists the beneficial properties of typical monomers for OH construction.

2. Photonic crystals hydrogels

Light can generate diffraction or surface plasmon resonance (SPR) at the interface of different media. The regular arrangement of different media can form a photonic band gap and make photons exhibit periodic changes in light intensity or wavelength^[33,34]. The photonic structures (gratings) of PCHs comprise regular arrangements between hydrogel matrixes and different block copolymers or polyelectrolyte layers. Specificity of PCHs is achieved by embedding receptors^[35,36] or building specific response structures. When the trigger conditions are met, PCHs have two response mechanisms:

- 1) PCHs made from functional hydrogels respond to physical (e.g., temperature, osmotic pressure, and magnetic field) or chemical (e.g., pH and salinity) stimuli. The stimuli cause changes in hydrogel volume and gratings. Thus, PCHs enable the detection of tested objects in the detection environment via wavelength monitoring, SPR, and even apparent color changes (**Figure 2a**)^[37,38].
- 2) Analytical targets bind to specific receptors on modified PCHs, transforming the electrostatic forces in the hydrogel grids. This transformation causes the expansion or contraction of the PCHs, changing the spacing of their internal gratings. The analytical targets can be accurately detected by monitoring wavelength variations, SPR, and even apparent color changes (**Figure 2b**)^[39,40].

Unmodified PCHs can detect some environmental indicators, such as temperature, humidity, and pH (**Section 2.1**). Incorporating specific chemical or biomolecular receptors in PCHs enables the detection of almost all common substances (**Section 2.2**). Moreover, constructing certain unique structures or introducing new technologies can further improve the detection accuracy of PCHs. PCHs have promising practical applications in disease diagnostics, biopharmaceuticals, pathogen screening, toxicity monitoring, and food security^[35]. Recently, they have been gradually introduced to environmental sensing.

2.1 Directly responsive photonic crystals hydrogels

Hydrogels that are responsive to one or more environmental stimuli can act as matrixes to build photonic crystal structures directly. The formed sensors are called directly responsive photonic crystal hydrogels (DR-PCHs), and have been used to detect humidity, pH, and temperature in the environment. Acrylamide glycol hydrogel and hydrogel synthesized from acrylamide (AAm) and acrylic acid (AAc) have high hygroscopicity; they shrink and swell at low and high humidity levels, respectively (**Figure 3a**). When constructed into regular photonic crystal structures, the changes in refractive index and apparent color induced by transformations in the hydrogel lattice constant can be used to detect environmental humidity^[41,42] (**Figure 3b**). Additionally, PCHs synthesized from 2-hydroxyethyl methacrylate (HEMA) and AAc respond to pH.

Monitoring their swelling rate enables the real-time detection of ambient pH^[43] (**Figure 3c**). Furthermore, PCHs constructed from the temperature-responsive polymer *N*-isopropylacrylamide (NIPAm) can detect temperature changes^[44].

DRPCHs, which are responsive to multiple environmental stimuli, are a notable research topic. They are formed by aggregating functional monomers with different stimuli-responsive properties. For instance, DRPCHs constructed from temperature-responsive *N,N*'-methylene acrylamide (BisAA) monomers and pH-responsive *N,N,N,N*-tetraethyl ethylenediamine (TEMED) monomers can simultaneously detect pH and temperature^[45]. In DRPCHs formed from temperature-responsive NIPAm monomers and glycidyl methacrylate (GAM) via a double crosslinking system, the primary amine groups of NIPAm and epoxy groups of GAM form a stable network structure. Besides temperature, these DRPCHs can detect alcohols via the destruction of the amine–epoxy bonds of the hydrogel by alcohols^[46] (**Figure 3d and 3e**).

Interestingly, some researchers have proposed a modular DRPCH synthetic method that enables polymerization of functional monomers around nanomagnetic particles (Fe₃O₄@polyvinylpyrrolidone) using a H-bond-guided template. These particles then aggregate under a magnetic field to form submicron photonic crystal chains (**Figure 4a**)^[47]. This modular preparation approach is universal, in the sense that these DRPCHs can aggregate monomers with various functions to respond to various environmental stimuli, and their submicron structure enables them to monitor the microenvironment. Although only pH-responsive chains have been produced through this method, the modularity and submicron structure aspects are particularly promising.

Some researchers have reported that besides environmental parameters, DRPCHs can potentially detect some microorganisms. For example, DRPCHs constructed with pH-sensitive hydrogels (HEMA–AAm polymer) shrink and expand depending on the pH, enabling the detection of acidic products from bacterial glucose metabolism (**Figure 4b**)^[48]. Furthermore, gelatin-based DRPCHs can be decomposed by gelatinase-producing bacteria, such as *Pseudomonas aeruginosa*. The swelling and decrease in crosslinking degree of DRPCHs under decomposed gelatin enable bacterial detection^[49]. Because carbohydrate and protein metabolism are widespread in microorganisms, DRPCHs for bacterial detection have no selectivity, along with low detection sensitivity. However, they provide a new direction for DRPCHs.

Overall, DRPCHs can hardly be used for the specific detection of pollutants. However, the stimuli-responsive capabilities of DRPCHs are the basis of most other types of PCHs and a critical bridge between object recognition and optical response in PCHs.

2.2 Photonic crystals hydrogels combined with receptors

Sensors known as receptor-bound photonic crystals hydrogels (RBPCHs) can be obtained by introducing compounds that specifically recognize pollutants into the hydrogel matrixes. Molecules contacting these sensors bind to the targets, affecting the hydrogel structure and thereby changing the wavelength of incident light and plasma.

2.2.1 Photonic crystals hydrogels with compounds receptors

As many compounds used to make RBPCHs have metal ion–chelating properties, these hydrogels have mostly been used for environmental heavy metal detection. For example, 3-arylamidopropyl-trimethylammonium chloride (ATAC) is a complexant for Cr⁶⁺ with hydrogel-forming properties^[50,51]. Aggregating ATAC, one of the hydrogel matrixes, with BisAA yields RBPCHs with good swelling properties. The formation of a complex between Cr⁶⁺ and the tertiary amine groups of ATCT affects the density and osmotic pressure of the RBPCHs. Cr⁶⁺ can thus be selectively detected by Bragg diffraction^[51] or SPR^[50] (**Figure 5a**). As they are anionic, ATAC-based hydrogels are sensitive to pH. Therefore, they require a continually maintained neutral test environment (pH 7).

The bidentate chelator 8-hydroxyquinoline (8-HQ), a quinoline derivative possessing two metal coordination groups (O covalent bond and N coordination bond) can chelate divalent and trivalent metal ions, such as Zn²⁺, Cd²⁺, Mg²⁺, Li²⁺, Mn²⁺, Co²⁺, Ni²⁺, Cu²⁺, Al³⁺, and Fe³⁺. Each metal ion chelated to 8-HQ

has specific O–metal and N–metal bond strengths (**Figure 5b**). Specific bonding between metal ions and coordination groups can change the grating structure in 8-HQ-based RBPCHs and modify their wavelength. Therefore, 8-HQ-based RBPCHs can be used to identify metal ions based on the wavelength and quantify them based on the changes in interference images caused by hydrogel volume changes^[52]. This complexation occurs even at extremely low metal ion concentrations, and the formed complexes will continue to chelate other 8-HQ molecules;^[53] thus, RBPCHs containing 8-HQ are extremely sensitive to metal ions. However, 8-HQ cannot form a hydrogel alone. Obtaining 8-HQ-containing RBPCHs requires using hydrogel matrixes with excellent swelling properties, such as poly(vinyl alcohol) (PVA), AAc, and polystyrene (PS)^[52,54] (**Figure 5c**). However, similarly to ATCT-based RBPCHs, 8-HQ-based RBPCHs rely on changes in osmotic pressure to detect targets. Therefore, the assay needs to be performed in a solution with certain osmotic pressure. Based on the same principle as ATAC- and 8-HQ-based RBPCHs, RBPCHs made from thiourea^[55] or dithiothreitol^[56] can specifically recognize Cd^{2+} and Hg^{2+} , respectively.

Instead of integrating ligand compounds directly in PCHs, grafting the target-interacting groups on hydrogel monomers can be a better strategy. For instance, RBPCHs containing NIPAm with crown ether groups as the side chains (CE-NIPAm) have a unique network structure. Their side chains can chelate Pb^{2+} ^[57,58] and Be^{2+} ^[59], and the main chains swell under the effect of electrostatic repulsion between the charged complexes and NIPAm backbone (**Figure 5d**)^[60]. Besides hydrogel swelling, metal–crown ether group polymers enhance the sensitivity of CE-NIPAM-based RBPCHs by affecting the osmotic pressure, as previously described. Therefore, the detection limit of CE-NIPAM for Pb^{2+} was as low as 10^{-9} M. The osmotic pressure of the hydrogel depends on the difference in ion concentration inside and outside the hydrogel; thus, this type of RBPCH needs to be kept in a solution with specific ionic concentration to achieve detection.

Besides metal ions, RBPCHs can detect certain small molecules. The amide groups of AAm undergo a methylation reaction with aldehydes in Na_2CO_3 solution, changing the chemical structure of the hydrogel. Thus, the RBPCHs constructed from AAm hydrogel can detect aldehydes via the apparent color changes caused by structural changes^[61]. When the RBPCHs are built from amine-rich hydrogel monomers, the amino groups from ionic liquids contact CO_2 gas and swell the hydrogel matrix. CO_2 gas can then be detected by monitoring the refractive index changes of the RBPCHs^[62].

2.2.2 Photonic crystals hydrogels combined with biomacromolecule receptors

It is difficult for RBPCHs with simple compound receptors to detect complex compounds or organisms. For these applications, enzymes, functional proteins, nucleotides, and DNA fragments are better receptor choices. Several RBPCHs with enzymes as receptors have been reported. A study with penicillin as the tested target^[63] directly introduced penicillinases as acceptors in AAm&AAc hydrogels. Penicillinases then hydrolyzed penicillin G to produce penicilloic acid. Electrostatic repulsion between the carboxylic acid groups of the hydrogel matrixes decreased with increasing pH. Periodic shrinkage of the RBPCHs under the change in osmotic pressure afforded penicillin G detection at very low concentrations (**Figure 6a**). Likewise, butyrylcholinesterase (BuChE) could decompose the sarin reagent (a highly toxic nerve agent) and generate hydrofluoric acid. When BuChE was immobilized into the AAm hydrogel matrix owing to an amide bond condensation reagent, the resulting RBPCHs could detect sarin with great sensitivity^[64].

For functional proteins, RBPCHs can exploit the well-known antibody–antigen recognition relation to detect microorganisms. Taking the rotavirus as an example, staphylococcal protein A can bind to immunoglobulins at non-antigen-binding sites. Staphylococcal protein A could be immobilized on a polyacrylamide (PAM) hydrogel with nanopores using silanol condensing agents. Subsequently, monoclonal rotavirus antibodies could be immobilized in the nanopores of this RBPCH to capture rotavirus. When the virus filled the nanopores, the refractive index of the RBPCH changed, enabling the detection of rotavirus^[65] (**Figure 6b**). Additionally, *Escherichia coli* could be indirectly detected by immobilizing polyclonal *E. coli* antibodies in RBPCHs using an immobilized biotin–streptavidin system. As a signal amplification system, each streptavidin molecule could bind four biotinylated antibodies^[66]. High-density loading of antibodies in hydrogels endows RBPCHs with high sensitivity for bacterial detection. Besides antibodies, RBPCHs directly constructed by pure lectin concanavalin A could detect *Candida albicans* owing to the polymer effect

between the glycoprotein mannan on the surface of *C. albicans* cells and concanavalin A^[67]. Glycated protein-functionalized RBPCHs can immobilize glycosyl groups on amino acid groups via nonenzymatic reactions. Hence, RBPCHs can detect Gram-negative bacteria by combining glycated proteins with lipopolysaccharides (D-glucosamine disaccharide, D-glucosamine, etc.) on the surface of bacteria^[68] (**Figure 6c**).

Moreover, to improve detection accuracy, some researchers have constructed ternary complex systems in RBPCHs^[69,70]. For example, RBPCHs based on the tryptophan (Trp)–Zn(II)–ciprofloxacin (CIP) ternary complex^[70] recognize and detect CIP owing to Zn(II)–CIP complex formation, which changes the osmotic pressure of RBPCHs. The amino and carboxyl groups of Trp were connected on the hydrogel backbone, and the exposed indolyl groups bound to Zn(II), forming a local positively charged region. When CIP was introduced as the target, Trp amplified the signal by exacerbating the osmotic pressure change (counterion effect) (**Figure 6d**), affording a CIP detection limit of 10^{-10} M. In contrast, in the tetracycline–Cu(II)–glycine (Gly) ternary complex system, the RBPCHs prepared by immobilizing tetracycline in the PAM matrix could detect Gly with high sensitivity^[69].

In summary, almost any biological or chemical reaction that can directly or indirectly cause structural changes in hydrogels can be used to build RBPCHs. The substances involved in the reaction can be regarded as detection targets and their receptors. Therefore, RBPCHs have a wide scope of development in pollutant detection. Any substance may become a receptor for a pollutant as long as a chain of “detection target–receptor–hydrogel structural change” can exist. This also means that RBPCHs could theoretically be constructed for the selective detection of any pollutant and even organisms.

2.3 Construction of photonic crystals hydrogels by inverse opal structures

PCHs come in many different structures, but the inverse opal structure is the most widely used (**Table 3**). PCHs with this structure can be called inverse opal-structured photonic crystal hydrogels (IOPCHs). They constitute regularly arranged nanoparticles as templates, and the voids are filled with high-refractive-index hydrogel matrixes. Removing the templates yields a symmetric and periodic structure with high porosity (**Figure 7a**)^[71]. When the refractive index of the medium filling the inverse opal structure reaches a certain value, complete photonic band gaps (PBGs) appear. Analytical targets change the PBGs of the IOPCHs, which can be detected by monitoring diffraction wavelength. Therefore, the most significant advantage of IOPCHs is that the PBGs can be easily controlled by adjusting the size and spacing of the templates.

In the preparation process, the most significant components of IOPCHs are templates, functional monomers, crosslinkers, and binding sites. PS and its functionalized particles are commonly used as templates (**Table 3**). Because PS can form highly ordered particle arrays via self-assembly at the gas–liquid interface, the array has a huge surface area and good crystal quality. More importantly, the size of PS (5 nm–5 mm) and space between the spheres can be easily tuned by plasmonic resonance;^[72] thus, the PBGs of PS-based IOPCHs are also easy to control. Besides, most IOPCHs use methacrylic acid (MAA), AAm, AAc, and their derivatives as functional monomers. Because these monomers can act as H-bond donors and acceptors and show good adaptability to ionic interactions, they are called “universal” functional monomers^[73]. As the crosslinking agent for functional monomers, BisAA enables hydrogels to undergo significant volume change under physical or chemical stimuli, which is key to the Bragg diffraction response during detection^[74].

Additionally, some IOPCHs without any receptor can also selectively detect targets. Replacing the filling medium of IOPCHs with tested targets with different refractive indexes transforms their PBGs. When the filling medium is air, the IOPCHs can detect solvents and gaseous molecules. For example, based on the differences in hydrogel swelling rates in different solvents, a PAM-based IOPCH encapsulating TiO₂ rapidly quantified different solvents using the PBG change^[75]. Gaseous molecules, such as H₂O₂^[76], toluene vapor^[77], acetone vapor, and ethanol vapor^[78], are rapidly adsorbed and diffused in the special porous structure of IOPCHs. The structure contains some media (dimethyl sulfoxide or air), and the PBGs of the IOPCHs migrate directionally when the targets replace the media (**Figure 7b**). Particularly, highly polar anions (e.g., SCN⁻) can form strongly hydrated ions. Hence, using water as a medium in IOPCHs inhibits H-bond formation between the hydrophilic group of IOPCHs and water, causing expansion of the material

and enabling SCN^- detection^[79].

Inverse opal structures can easily form dense nanophotonic crystals and synchronously modify various specific receptors by self-assembly. The ample nanopores allow high receptor density and target capture capability. Therefore, the detection sensitivity of IOPCHs is usually higher than that of PCHs with other structures.

2.4 Application of molecular imprinting technique in photonic crystals hydrogels

Molecular imprinting-based PCHs (MIPCHs) can detect targets without corresponding receptors with high recognition accuracy. The targets serve as templates during the assembly of the functional monomers via covalent/noncovalent interactions. Removal of the imprinted molecules leaves a “blot”, conferring MIPCHs with the ability to selectively detect the corresponding objects^[80,81] (**Figure 8a**). These imprinted molecules can be metal ions^[82,83], compounds^[84-87], and even organisms^[68]. Ions cannot usually be direct template molecules for MIPCHs, and imprinting them into the hydrogel grid requires the assistance of certain complexes. For instance, in 5'-O-acryloyl-2',3'-O-isopropylidene guanosine (APG)-modified MIPCHs, Sr^{2+} induces the formation of planar G-quartets by APG units. After removing the Sr^{2+} templates, the cavities remaining in the hydrogel network provide accurate binding sites for Sr^{2+} . Upon reexposure to Sr^{2+} , APG-modified MIPCHs shrink due to the weakened electrostatic repulsion between the four O atoms in the relaxed G-quadruplex^[82] (**Figure 8b**). Similarly, pentaethylenhexamine (PEHA) can coordinate with Pb(II) to form an imprint. MIPCHs formed from secondarily crosslinked Pb(II)-treated pentaethylenhexamine and a PAM hydrogel detected Pb(II) with high sensitivity^[83]. Besides, with MIPCHs, some compounds can directly act as imprinted molecules. For example, tetracyclines used as a template molecule increased the hydrogel crosslinking degree of MIPCHs formed from AAm^[84] or AAc^[85]. When the imprints were secondarily bonded with tetracyclines, the MIPCHs could detect tetracyclines via changes in the hydrogel crosslinking degree (**Figure 8c**).

Notably, almost all MIPCHs have adopted the inverse opal as the photonic crystal structure because molecular imprints can be densely and evenly imprinted in this 3D-ordered-nanochannel structure. Imprinted molecules branded with specific receptors can greatly improve the detection sensitivity of RBPCHs. In a previous report^[68], PCHs containing glycosylated proteins imprinted with *E. coli* exhibited 2.67 times in *E. coli* detection sensitivity, compared with the PCHs without imprinting.

All these structural techniques for PCHs are not independent: combining them affords better performance. In the face of increasingly complex environmental pollutants, PCHs combining multiple detection approaches may be one of the most promising development directions of OH-based environmental pollutant detection technologies.

3. Fluorescence hydrogels

Fluorescence is a typical photoluminescence phenomenon. When fluorophores absorb high-energy light, their electrons enter the excited state from the ground state, then release energy in the form of light emissions^[88,89]. Fluorescence-based detection technologies have the advantages of high sensitivity, high selectivity, and convenience^[90]. Hydrogels have porous junctions, excellent biocompatibility, and highly controllable physicochemical properties. Therefore, introducing fluorophores into hydrogel matrixes yields sensors combining the advantages of both materials that have broad application potential in bioimaging, medical diagnosis, pollutant detection, and gene technologies^[90,91]. These hydrogels can be called fluorescent hydrogels (FHs). When analytical targets contact FHs, the fluorescent modules respond through five main pathways:^[92,93] photoinduced electron transfer (PET)^[94], intramolecular charge transfer (ICT)^[95], excited-state intramolecular proton transfer (ESIPT)^[96], fluorescence resonance energy transfer (FRET)^[97], and excimer/excimerplex interaction^[98] (**Table 4**).

3.1 Hydrogels loaded with compound fluorophores

In compound fluorophore hydrogels (CFHs), the turn-on system comprising compound fluorophores and hydrogel matrixes is the most typical, and is based on the PET principle. For instance, the well-known rhodamine fluorophore can be grafted onto oxidized agarose via a carboxyl-amine reaction^[99], and the

modified oxidized agarose can be oxidatively polymerized directly with AAm from CFHs^[100]. At that moment, the formed spirocyclic lactam structure in the CFHs quenches the fluorescence. After binding to the targets (Pb^{2+} and Al^{3+}), the CFHs convert to the ring-opened amide structure and generate pink (Pb^{2+}) or yellow (Al^{3+}) fluorescence (**Figure 9a–b**). Besides their use as a fluorescence “switch,” hydrogel matrixes can condense fluorophores and amplify the detection signal by shrinkage^[99], yielding detection sensitivities of 10^{-7} M and 1.5×10^{-6} M for Pb^{2+} and Al^{3+} , respectively. Likewise, 3D porous frameworks with abundant H-bond donors and acceptors, constructed using sodium alginate (SA), can combine with 9-anthraaldehyde via the supramolecular Cu coordination polymer Cu-atda and form CFHs. The differences in electron energy levels between 9-anthraaldehyde/Cu-atda and different antibiotics (flumequine and nitrofurans) causes electron transfer between them. Thus, multiple antibiotics can be detected via fluorescence quenching or enhancement^[101].

Moreover, the fluorescence of boron-dipyrromethene (BODIPY) is quenched when its pyridine groups are complexed with the Co core of cobaloxime. HS^- can replace the pyridine group to generate HS–cobaloxime, restoring isolated BODIPY fluorescence(**Figure 9c**). Besides, polyurethane can capture and ionize H_2S gas into HS^- . Thus, CFHs comprising BODIPY, cobaloxime, and polyurethane enable the detection of gaseous H_2S ^[102]. Meanwhile, when BODIPY was introduced to the symmetrical thiophene aldehyde groups and grafted on chitosan, the formed CFHs enabled Cu^{2+} detection, as Cu^{2+} quenched the fluorescence of the modified BODIPY^[103] (**Figure 9d**). Notably, the electron distribution changes within BODIPY are influenced by pH changes and cause a red/blue shift of fluorescence (ICT principle). Therefore, BODIPY-based CFHs can be used to detect pH^[104,105] or NH_3 ^[106]. CFHs based on the ICT principle are another major type of hydrogel. Typically, morin and the Al^{3+} of hydrotalcite (MR–HT) form a stable electron cloud and emit fluorescence. HPO_4^{2-} or H_2PO_4^- can rob Al^{3+} and change the fluorescence properties of MR–HT by internal electron rearrangement (**Figure 9e**). Hence, CFHs comprising polyurethane and MR–HT can detect HPO_4^{2-} and H_2PO_4^- with high sensitivity. Besides, polyurethane prevents fluorophore leakage, and its polarity increases the sensitivity of MR–HT to PO_4^{3-} ions^[107].

Moreover, some CFHs detect pollutants through the ESIPT principle. For example, *N*-(3-(benzo[d]thiazol-2-yl)-4-(tertbutyldiphenylsilyloxy)phenyl)acetamide (BTBPA) can be isomerized to *N*-(3-(benzo[d]thiazol-2-yl)-4-hydroxyphenyl)acetamide (BTHPA) with a longer fluorescence wavelength by cleaving the Si–O bond using F^- (**Figure 9f**). Thus, a BTBPA-immobilized poly(*N*-vinyl-2-pyrrolidone) hydrogel detected F^- , and the strong adsorption and diffusion of F^- by poly(*N*-vinyl-2-pyrrolidone) afforded a detection time of only 15 s^[108]. Based on the same mechanism, 2-hydroxy-1-naphthaldehyde was introduced into the amino side chain of chitosan and aggregated into a CFH. This CFH achieved Cd^{2+} detection as the direct bonding of Cd^{2+} to the hydroxyl and imine groups of chitosan caused the tautomerism of fluorophores and quenched the fluorescence(**Figure 9g**)^[109].

Fluorescent pyrenes with chiral aromatic amino acid amides can bind oligo oxyethylene chains through gallic acid anchors to form CFHs without hydrogel matrixes. ClO^- detection was achieved as acyl aroyl hydrazine units of the CFHs were selectively oxidized, changing the fluorescence of pyrene (**Figure 9h**). Changing the anchors and groups attached to the pyrenes would allow the detection of other oxidizable substances. However, this hydrolysis caused a sol reaction, which was detrimental to the stability of the CFHs^[110]. Interestingly, 8-HQ, described in Section 2, is weakly fluorescent, and complexes between 8-HQ and metal ions can enhance the fluorescence by blocking the ESIPT channel^[111]. Therefore, PCHs with 8-HQ as an acceptor could detect metal ions more sensitively with the assistance of a fluorescence enhancement system (**Figure 9i**). Different metal ions could also be identified owing to their ESIPT-blocking ability^[54].

Finally, some CFHs achieved pollutant detection by quenching the fluorescence of unstable complexation to ions. Therefore, some ions can be detected by repeatedly breaking and recovering unstable complexes. For example, salicylaldehyde (SD) and thiosemicarbazide (TB) can form a p– π conjugated system, with their respective unsaturated conjugated chains connected to electron-poor and electron-rich groups. The SD–TB complex fluoresces via electron transfer at specific excitation wavelengths. CFHs constructed on this basis can detect Cu^{2+} via fluorescence quenching owing to the transfer of Cu^{2+} electrons to the fluorophore.

More importantly, Cu^{2+} captured by the CFHs could be extracted under the action of chelating agents (ethylenediaminetetraacetic acid) to restore fluorescence (**Figure 9j**). Therefore, the Cu-complexed SD–TB hydrogel could also detect compounds with metal-chelating properties^[112]. Based on the same “on–off–on” mechanism, CFHs loaded with R19S fluorophores were used for the repeated detection of Hg^{2+} ^[113] (**Figure 9k**). In these CFHs, along with specific functions, the hydrogel matrixes played the role of dispersing and immobilizing fluorophores and preventing contamination of the sensors.

3.2 Hydrogels loaded with biomacromolecules

Highly editable biomacromolecule fluorophore hydrogels (BFHs) were created to exploit the fact that embedded proteins and DNA can maintain their native structures and functions owing to the high-water content and excellent biocompatibility of hydrogels. BFHs embedded with functionalized DNA are the most common. The fluorophore SYBR Green I emits weak fluorescence when linked to single-stranded DNA (ssDNA). Meanwhile, its fluorescence dramatically increases when it binds to double-stranded DNA (dsDNA), and the intensity is related to the amount of dsDNA (FRET principle). Hg^{2+} can then promote the transformation of ssDNA to dsDNA with a hairpin structure by inducing base pairing between thymine and thymine (**Figure 10a**). Hydrogel matrixes (such as polyacrylamide and agar) with immobilized thymine-containing ssDNA and SYBR Green I thus enable Hg^{2+} detection^[114–116] (**Figure 10b**). Hydrogel matrixes prevent leakage of the DNA–fluorophore system, and their strong adsorption of Hg^{2+} affords highly sensitive detection.

Similarly, Cu^{2+} can bind to thymine, but thymine-complexed Cu^{2+} can be reduced by a reducing agent (such as ascorbic acid) into Cu^0 , which has a particle size close to single Cu atom. Cu^0 then forms Cu nanoclusters (NCs) that emit red fluorescence (FRET principle). Based on this, polythymidine DNA (PT-DNA) immobilized on agar can emit fluorescence and portably detect Cu^{2+} without additional fluorophores^[117]. Moreover, when introducing both Hg^{2+} and Cu^{2+} into BFHs, PT-DNA tended to combine with Hg^{2+} first. If a compound with stronger affinity for Hg^{2+} entered the BFHs, Cu^{2+} would combine with PT-DNA, form Cu NCs, and emit fluorescence^[118]. Hence, these BFHs can be used to detect some metal chelators. Moreover, more complex PT-DNA-based BFHs have also been reported. Tyrosinase had an enzyme-controlled quenching effect on the fluorescence of Cu NCs, and organophosphorus compounds could inhibit tyrosinase and recover fluorescence. Therefore, PT-DNA-based BFHs combined with tyrosinase enabled pesticide detection^[119]. Based on similar mechanisms, higher-cost DNA-templated fluorescent Au NCs^[120] and Ag NCs^[121] could also detect different pollutants.

Owing to the inherent advantages of DNA technologies for microbial detection, DNA-based BFHs were mostly used to detect environmental pathogenic microorganisms. For viruses, one end of the target virus (e.g., HIV, HCV, SARS, or H5N1) sequences (ssDNA) was immobilized on hydrogel matrixes by amino groups, and another end was modified with a fluorophore. The modified ssDNA hybridized with fully complementary fluorescence-quenching strands to form dsDNA. When the target virus entered the BFHs, they combined with the quenching strands, restoring fluorescence (**Figure 11a**)^[122,123]. Although reverse transcription loop-mediated isothermal amplification (RT-LAMP) is simple, scalable, widely applicable, and does not require complex microbial equipment^[124], the complexity of environmental samples often affects the detection of viruses. When RT-LAMP-based reagents were crosslinked with the microporous track-etched polycarbonate membranes through polyethylene glycol (PEG) monomers, impurities in the sample were filtered out or adsorbed by the special polycarbonate membrane^[125]. This technique enabled accurate on-site detection of viruses (SARS-CoV-2). In the above two examples, the hydrogel matrixes used embedded ssDNA in a highly dispersed state to enhance nucleic acid hybridization rates. Their dense microporous structure and rich groups filtered out some impurities in the samples and enhanced the adsorbability to viruses. Therefore, the sensors exhibit excellent antifouling performance and detection efficiency^[126,127].

DNA-based BFHs also work for bacterial detection. For example, fluorescence probes and specific bacterial (*E. coli*) recognition ssDNA strands were immobilized on arrayed 3D hydrogel chips. When the chips were placed in bacterial lysis fluid, the polymerase chain reaction (PCR) was started directly without the DNA template extraction procedure, and the resulting fluorescence signal was immediately detectable^[128]. Therefore, the required inspection time was significantly reduced. Interestingly, a similar mechanism was

used for detecting some biological toxins. Rolling circle amplification reaction primers were hybridized with ochratoxin A aptamers to form partially complementary dsDNA. Aptamers can bind to ochratoxin A, releasing the primers and enabling ochratoxin A detection. The separated primers combined with the padlock probe to form a circular template and started the rolling cycle amplification reaction under enzymatic action. The rolling cycle amplification products wrapped fluorophores to form DNA hydrogels, and the polymerization process made the dispersed fluorophores continue to aggregate (**Figure 11b**). There was a positive correlation between fluorescence intensity and ochratoxin A concentration^[129].

Unlike DNA-based BFHs, BFHs containing biological enzymes can sensitively detect pollutants without complicated biomimetic procedures. Typically, BFHs containing acetylcholinesterase (AChE) enable the detection of residual pesticides (paraoxon^[130], carbaryl^[131], and organophosphorus^[132]) and insecticides (dichlorvos^[133]) in the environment via various mechanisms: (1) BFHs with immobilized AChE and quantum dots (QDs) could detect paraoxon because *p*-nitrophenol, produced from the reaction between paraoxon and AChE, quenched the fluorescence of QDs;^[130] (2) H₂O₂ produced by BFHs containing AChE and choline oxidase quenched the fluorescence of QDs, and the combination of dichlorvos with AChE prevented H₂O₂ production, enabling dichlorvos detection;^[133] (3) AChE produced thiocholine via hydrolysis, quenching the fluorescence of QDs by complexing with Ag²⁺ or triggering the fluorescence of upconversion nanoparticles by hindering dopamine polymerization^[131,132]. In all these systems, pesticides inhibit AChE, which affects fluorescence. Similarly, dichlorvos can be detected by BFHs equipped with a Cu²⁺-AChE-carbon dot (CD) system^[134]. Besides, BFHs containing tyrosinase-QD conjugates can also emit bright orange fluorescence. Quinone intermediates generated by the catalytic oxidation of tyrosinase to phenol and its derivatives can act as electron acceptors and quench fluorescence (FRET principle)^[135-137]. Hence, these BFHs detected phenol and its derivatives with high sensitivity.

In enzyme-based BFHs, enzymes need to cooperate with fluorophores (e.g., CDs and QDs) and other substances (e.g., choline oxidase and Ag²⁺) to detect pollutants. The hydrogel matrixes are not directly involved in the detection, but can make each substance in the detection system extremely uniformly dispersed. These sensors have fast fluorescence responses, and the consistency and stability of fluorescence response across the sensor is guaranteed. Additionally, enzyme-based BFHs can target adsorption and antifouling. Besides enzymes, peptide sequence-based BFHs can also detect pollutants. When polypeptides modified with fluorophores were immobilized on dispersed tetraphenylethylene, organophosphorus could covalently bind the serine of peptides, forcing their aggregation and the gelation of tetraphenylethylene. The resulting fluorophore aggregation increased fluorescence intensity^[138]. This was a special mechanism as the hydrogel no longer acted as a matrix, but the polymerization process of hydrogel monomers was used to gather free fluorophores and enhance fluorescence instead.

In BFHs, biomacromolecules usually cannot emit fluorescence directly. However, as the bridge between targets and fluorophores, they play the role of capturing targets and controlling fluorescence. This mechanism is similar to that of RBPCHs, but BFHs are usually more scalable and editable, and their sensitivity and specificity are higher. However, because of their technological complexity, BFHs are currently more commonly used in cell diagnosis, immunoassays, and medical diagnosis^[139-141] rather than pollutant detection.

3.3 Quantum dots loaded in the hydrogels

QDs are colloidal semiconductor nanocrystals measuring between 1 and 10 nm. Their fluorescence is generated by electron-hole recombination upon irradiation with excitation light^[142]. QDs have bright fluorescence, photostability, excellent multiplexing ability, and their emission wavelength can be controlled by modulating crystal size and material properties^[143,144]. Presently, QD fluorescent hydrogels (QDFHs, made by combining hydrogel matrixes with CDs, graphene quantum dots (GQDs), silicon quantum dots (SiQDs), and enzyme QDs have been used for environmental pollutant detection.

3.3.1 Carbon dots

CDs have stable fluorescence without additional excitation conditions; thus, analytical targets can be detected only if they quench or enhance fluorescence. Besides, CDs contain abundant carboxyl groups, affording them

good water solubility and compatibility with various organic substances, polymers, inorganic substances, and even biomolecules^[145] (**Figure 12a**). Compared with expensive precious metal or heavy metal-based QDs, which are potential environmental and biological hazards, CDs have low cost, abundant sources, low toxicity, and good biocompatibility^[145,146]. The applications of CDs in environmental pollutant detection have been reported the most and demonstrate great potential.

The most notable property of CDs is that their fluorescence can be directly and significantly quenched by metal ions^[147]. Therefore, metal ions can be quantitatively detected owing to their direct fluorescence quenching of CDs. This property is most commonly used by FHs with CD fluorophores (CDFHs). Cellulose nanofibrils (CNFs) are an ideal material for hydrogel matrixes^[148-154] of CDs aiming to detect metal ions (e.g., Cr^{6+} , Fe^{3+} , Ba^{2+} , Pb^{2+} , Cu^{2+} , and Hg^{2+}). They possess nanoscale size, strong stiffness, high specific surface area, and special 3D network structures^[155,156]. The porous structure of CNFs endows CDFHs with many CD and metal ion-binding sites. Besides, they have great fluorescence quantum yield, density, and adsorption capacity for heavy metal ions (**Figure 12b**). Hence, CNF-based CDFHs not only have excellent detection abilities for heavy metals but can also adsorb heavy metal pollution^[148,151,157]. More importantly, all C-rich materials are theoretically sources for CDs and CNFs. CNF hydrogel precursors and CDs can be generated simultaneously from biosourced materials via one-pot hydrothermal methods^[158,159]. This method is cheap and nontoxic.

Notably, hydrogel matrixes prepared from single natural CNFs have various drawbacks, such as poor flexibility and environmental adaptability. To overcome this, CDs–CNFs were crosslinked with other hydrogel matrixes, including AAm&AAc^[151,153], chitosan^[148], polyethyleneimine (PEI)^[149], and epichlorohydrin^[150]. In these materials, the abundant amino groups provided by chitosan can couple with sulfonic acid. Chitosan-based CDFHs combined with molecular imprinting technology enable the detection of perfluorooctanesulfonic acid (PFOS)^[160]. Furthermore, PEI can be used as a N-rich surface passivator to modify CDs (N doping) and improve the fluorescence quantum yield and performance^[149,161]. In CDs treated with PEI (PEI-CD), ClO^- oxidized the phenol groups of PEI-CD into benzoquinone groups and quenched fluorescence via the ICT principle (**Figure 12c**). Hence, this system allowed specific ClO^- detection^[162]. Besides PEI and its derivatives, some compounds, such as urea^[152,163] and ethanediamine^[148,164], could also be used as N dopants.

CDFHs were also used to detect antibiotics (such as tetracycline^[165-167] and rifampicin^[168]). All of these studies have shown that the absorption spectra of antibiotics and the excitation spectrum of CDs have enough overlap to cause fluorescence quenching. Some researchers attributed this to the inner filter effect (IFE) between antibiotics and CDs^[166,167]. Others attributed it to the FRET effect caused by the combination of antibiotics and surface functional groups of CDs^[165,168].

CDFHs also show potential for bacterial detection. When amphiphilic CDs were assembled into the hydrogel matrixes constructed using 6-*O*-acylated fatty acid esters, the esterase secreted by bacteria cleaved the ester bonds, making the hydrogel network collapse. This collapse caused CD aggregation, which quenched fluorescence and enabled bacterial detection^[169] (**Figure 12d**). Finally, CDFHs can be used to measure pH. The surface functional groups (amino, amide, carbonyl, and carboxyl groups) of CDs undergo reversible protonation and deprotonation based on pH. When the valence bands of CDs are filled or depleted, the fluorescence intensity and emission peaks change^[170,171] (**Figure 12e**). Because CDs exhibit stable fluorescence, the tested targets only affect the fluorescence intensity and hardly change the fluorescence properties. Therefore, CDFHs can recognize multiple targets simultaneously, but they usually lack specificity for targets without the help of additional recognition modalities, particularly for detecting metal ions. Most metal-detecting CDFHs have been used as indicators for metal-adsorbing materials.

3.3.2 Graphene quantum dots

As a special kind of CD, GQDs have a layered structure and good crystallinity, and can therefore provide higher quantum yields than CDs and exhibit excellent trapping properties for photons in the short-wavelength region^[172,173]. Additionally, as giant polycyclic aromatic hydrocarbon molecules, GQDs have complex chem-

ical groups, functional groups, defects, and dopants^[174] (**Figure 13a**). These unique properties can also be controlled by changing the size of graphene, disrupting the integrity of the π -electron system, and adjusting the chemical or layered structure^[175]. Therefore, the first QD-based FHs (GQDFHs) attracted widespread attention in medical areas, such as drug delivery, bioimaging, and in vitro diagnostics^[176]. Their application to environmental pollutant detection has just begun.

For example, QDs were crosslinked with reduced graphene oxide to form porous 3D GQDFHs via multilayer H-bonding. Reduced graphene oxide adsorbed U^{6+} via strong complexation, while coordination interactions between the O and N groups of QDs and U^{6+} quenched the fluorescence. These two phenomena enabled sensitive U^{6+} detection sensitively^[177]. Similarly, glyceryl methacrylate-functionalized QDs were crosslinked with polythioctic acid, BisAA, and gelatin to form GQDFHs. These GQDFHs adsorbed Cd^{2+} and Pb^{2+} via coordination with C–S bonds and chelation with thiol groups and enabled the detection of these metal ions via IFE-based chelation-enhanced fluorescence or chelation-quenched fluorescence^[178] (**Figure 13b**).

Besides metal ions, the PN junction synthesized from Ni^{2+} and histidine-functionalized QDs to form GQDFHs with PVA could oxidize 3,3',5,5'-tetramethylbenzidine and quench the fluorescence. Lambda-cyhalothrin blocked this process by inhibiting the activity of the PN junction, enabling detection^[179]. Besides, graphitic carbonitride QDs encapsulated into 3D GQDFHs have much higher fluorescence intensity than ordinary QDs. With the assistance of biological aptamers (specificity dsDNA), these 3D GADFHs enabled the selective and sensitive detection of kanamycin^[180] and even *E. coli*^[181]. These examples show that the complex organic structure of QDs endows GQDFHs with strong scalability and different expansion possibilities. As one of the newest nanomaterials, GQDFHs are one of the most promising pollutant detection sensors, even though few reports on their application in environmental pollutant detection exist.

3.3.3 Other QDs

Besides the above two QDFHs, SiQDs have fluorescence properties similar to those of CDs as well as low toxicity and good biocompatibility^[182,183]. Based on the same fluorescence suppression mechanism, QDFHs containing SiQDs have been used to detect metal ions (such as Cr^{6+} , Fe^{3+} , or Cu^{2+})^[184,185]. Additionally, the QDs in the aforementioned Ag^+ -AChE-QD system for detecting organophosphorus and paraoxon were SiQDs^[130,132]. Meanwhile, SiQDs synthesized chemically using Si solution possess hydrogel properties and can form QDFHs even without the aid of hydrogel matrixes. Using hydrogel monomers only improved the sensor performance, such as its strength and flexibility. More importantly, SiO_2 hydrogels can efficiently be turned into aerogels through various drying methods; thus, SiQD-based fluorescent aerogels are conceivable. This could potentially enable air pollutant detection, which most OHs cannot do, but there have been no reports on this so far.

Cd-based QDs (CdQDs) were the earliest reported QDs, and many types of CdQD-based FHs have been developed to detect various pollutants. For example, NO_3^- anions can bind to positively charged PEI-CdS QDs and be detected via the resulting fluorescence quenching during electron transfer (ESIPT principle)^[186,187]. Meanwhile, cations (H^+ and Fe^{3+}) could be captured by the negatively charged carboxyl groups of SA hydrogels and detected by CdS immobilized in the hydrogels^[188]. A QDFH with CdTe QDs in a QD-AChE system could detect organophosphorus without the coordination of metal ions, unlike other AChE-based FHs (**Section 3.2**)^[189]. Besides, CdSe/ZnS cooperated with specific dsDNA to realize virus detection^[123], and carboxylated Cd-based QDs were also used to detect phenols via a tyrosinase-QD system^[135-137]. The commercialization of various CdQDs enabled the easy preparation and even mass production of CdQD-based FHs for different detection targets. However, the potential environmental and health hazards of heavy metal-based QDs have been worrisome, even though the hydrogel matrixes have prevented the leakage of heavy metal ions to a certain extent.

3. 4 Living luminescent microorganisms immobilized in hydrogels

The unique sensor formed by immobilizing natural or artificial living luminescent microorganisms in hydrogel matrixes can be called bioluminescence hydrogels (BLHs). They are mainly used for toxicity detection. Toxicity is the damage caused by xenobiotics to organisms; it involves biochemical processes that are com-

plex, hard to elucidate clearly, and difficult to simulate in vitro. It also involves the uniform expression of complex mixtures in polluted environments. Currently designed sensors based on chemical and physicochemical processes can detect most environmental pollutants, but all the previously described strategies for OH design were unable to evaluate pollutant toxicity. However, the implantation of living luminescent microorganisms can allow OHs to detect toxicity. The stable grid structure, mechanical strength, and high hydrogel biocompatibility allow living cells to be confined within the hydrogel grids and maintain their original activities^[29,190].

Furthermore, the porous structure of hydrogels is an excellent environment for cell attachment and proliferation. It provides ample space for cell growth, while the rich functional groups facilitate the transport of metabolites and nutrients in and out of the capsules^[191,192]. More importantly, it is also feasible to add nutrients in hydrogel matrixes to maintain the long-term activity of microorganisms because of the similarities between hydrogels and water. Finally, the antifouling and adsorption properties of hydrogels described above make BLHs more resistant to environmental disturbances and more sensitive to targets than 1 unimmobilized living luminescent microorganisms. All of these unique properties enable the construction of toxicity sensors.

Living luminescent microorganisms include natural luminescent bacteria and genetically recombinant bacteria. Natural luminescent bacteria include *Vibrio fischeri*, *Vibrio harveyi*, *Pseudomonas fluorescens*, and *Pseudomonas leiognathid*. Toxic substances can affect their cellular metabolic states and quickly suppress their luminescence intensity^[193], making them useful for evaluating the acute toxicity of samples. For example, *V. fischeri* immobilized in a PEG diacrylate hydrogel to form test paper enabled the quick assessment of water toxicity^[194]. *Pseudomonas leiognathid* immobilized on agar, carrageenan, and SA was used to test heavy metal and pesticide-associated toxicity in water systems. These studies showed that SA-based BLHs performed best^[195]. Besides, as a natural anionic polymer, SA has high biocompatibility, and its crosslinking process is mild and nontoxic. Therefore, using SA to encapsulate cells provides the highest benefits for biological application^[196,197]. The same goes for BLHs.

For genetically recombinant bacteria, *E. coli*^[198,199] and yeast^[200,201] are the two most common host cells. They were implanted with low-transcript plasmids that contained a transcribed fusion gene of the green fluorescent protein and an antibiotic resistance gene. The region between two adjacent open reading frames on the plasmids was amplified and embedded with different promoters for stress-related genes (**Figure 14a**)^[202,203]. When the stress conditions of the promoters were reached, the corresponding gene channels opened to drive the expression of the fluorescent protein gene, and the bacteria thus emitted specific fluorescence. In toxicity assays, these stress genes were associated with oxidative stress, protein stress, detoxification, electron transport, and DNA damage^[198,199]. However, the possible escape of genetically recombinant bacteria during testing and diffusion of their unnatural genes in natural microbial systems, especially antibiotic resistance genes, is worrisome^[204,205]. Immobilization of genetically recombinant bacteria on hydrogel matrixes can effectively prevent the leakage of bionts and their unnatural genes. For example, a directionally designed genetically recombined *E. coli* embedded in SA hydrogels enabled the quantification of 2,4,6-trinitrotoluene via the toxicity response^[206] (**Figure 14b**).

Interestingly, under the action of the gas-liquid interface and organic matter adsorption effect of SA, BLHs embedded with *E. coli* could detect formaldehyde, cigarette smoke, acetone, and other toxins in the gas phase^[207,208]. To further prevent the leakage of genetically recombinant bacteria and their unnatural genes, researchers constructed a hard BisAA shell outside the *E. coli*-embedded SA hydrogel core (**Figure 14c**). However, this process did not compromise the sensitivity of the sensor to heavy metals in real water^[18]. Additionally, *E. coli*, embedded in PEG diacrylate (with better mechanical strength than SA)^[209] or agar (without chemical crosslinking)^[210,211] enabled the detection of environmental toxicity in water. Agar-embedded *E. coli*-based BLHs were used for continuous monitoring and early warning of water toxicity. However, the leakage of genetically recombinant bacteria that were not restricted by the crosslinked chemical network could easily cause new environmental concerns.

Presently, there are few reports on BLHs, but their special detection properties could not be achieved by other OH sensors. Solving biological leakage, stability, and long-term storage problems will make BLHs

particularly attractive for environmental pollutant detection.

4. Other optical hydrogels for environmental sensing

Light diffraction-based PCHs and fluorescence-based FHs have accounted for almost all the existing studies using OHs for environmental sensing. There are few reports about sensors based on OHs that are neither PCHs nor FHs and are not aimed at pollutant detection in the environment. This section briefly discusses some of these OHs.

In some studies, hydrogels with specific stimulus responsiveness were wrapped at the end of the fiber to form the interference structure. When the stimulation conditions were reached, the expansion or contraction of the hydrogel changed the wavelength of light in the fiber^[212-215], enabling target detection (**Figure 15a**). For example, ambient humidity could be measured by the interference structure of optical fibers wrapped with a strongly hygroscopic hydroxypropyl methylcellulose hydrogel^[215]. Additionally, fibers coated with DNA aptamer-modified^[212] or glucose recognition agent-doped^[213,214] hydrogels enabled the detection of more complex targets, such as K^+ and glucose. In another method, hydrogel films with specific stimulus-responsiveness covered the surface of a metal sensor with a glass substrate to make an optical waveguide structure. When the stimulation conditions were reached, the changes in hydrogel film volume affected the refractive index of the incident laser, ultimately changing the waveguide spectra^[216-218] (**Figure 15b**). Likewise, when the hydrogel film was pH-sensitive, the optical waveguide sensor could detect pH^[216], and when a streptavidin system was added to the film, the sensor could detect bacteria^[217]. Sensors with waveguide-structured hydrogels could also detect biomolecules with more complex designs. For instance, a terpolymer hydrogel layer doped with estradiol monoclonal antibody was covered on a laser prism with gold film. When contacting estradiol molecules, the refractive index changes were detected through plasmon resonance-excited optical waveguide modes^[218]. Particularly, some researchers made Fresnel lenses from pH-sensitive hydrogels using the replica mold method. Changes in focal length and focusing efficiency caused by changes in hydrogel volume enabled pH detection^[219] (**Figure 15c**).

Overall, the basic detection mechanism of these sensors is similar to that of PCHs. The target affects the hydrogel volume, generating detectable plasma resonance, refraction, or diffraction changes. In both fiber-based and optical waveguide-based OHs, the hydrogel matrixes are just the auxiliary structures of various optical devices (fiber optics, laser transmitters, signal receivers, precious metal resonance films, prisms, glass baseboards, etc.). These hydrogel-assisted optical sensors may have advantages for developing wearable flexible detection devices. However, optical waveguide or optical fiber detection equipment may have insufficient reliability and sensitivity for pollutant detection. Besides, they are far less convenient, cheap, and efficient than PCHs, which can become rapid detection kits without additional equipment. Compared with PCHs and FHs, most other OHs have no advantages or applicability in environmental sensing. Therefore, the next section only discusses and analyzes PCHs and OHs.

5. Perspective of optical hydrogels for environmental sensing

Compared with other contaminant detection methods, the most significant advantages of OHs are portability, rapidity, and low detection cost. However, for any detection technique, the detection sensitivity and variety of detectable objects are the most critical metrics. Therefore, after classifying and discussing the various types of OHs, we performed statistical analysis on 138 papers extracted from the literature that clearly documented the limits of detection (LODs) for different pollutants.

5.1 Detection performance analysis

As reported in the selected papers, OHs can detect heavy metals, anions, antibiotics, pesticides, small organics, gas molecules, environmental parameters, and microorganisms in the environment (**Figure 16a**). Additionally, OHs can detect much more targets such as anesthetics in fish^[220], metabolites of microorganisms in complex media^[221], melamine in milk^[222], and catecholamines in serum^[223]. These examples indicate that OHs have broad potential for detecting increasingly complex contaminants in the environment, and this field needs more research.

To further explore the sensitivities of different OHs in different kinds of contaminant detection, we extracted the LODs of OHs for different targets from 138 papers and compared them with the reported LODs of standard detection methods (**Table 5**). We calculated the normalized sensitivities as $Q = L_o/L_s$, where, L_o represents the LOD for a certain pollutant using a certain OH, L_s represents the LOD for this pollutant with the standard method from China, the USA, Australia, the UK, or the International Organization for Standardization. $Q < 1$ indicates more sensitivity than the standard method, and *vice versa*. We processed the Q values with the TRIMMEAN (percent = 22%) function to reduce the impacts of outliers. We transformed normalized data into a natural logarithmic function form and plotted the results as a heatmap (**Figure 16b**).

Overall, the PCHs had higher normalized sensitivities for pollutant detection than FHs because all the PCHs are nanoscale grating structures that can reflect any tiny change caused by the targets. Additionally, the target receptors can be directly grafted on the gratings by the hydrogel backbones. PCHs are both target recognition and signal expression units, without the need for “bridges” for signal transmission. However, in FHs, the fluorescence and target recognition units usually exist separately, and the signal needs to be converted and transmitted via one or more steps. Therefore, the density, uniformity, coordination of fluorophores and acceptors, and complexity of signal transmission may all affect the sensitivity of FHs.

Next, we analyzed the detection sensitivities of each OH for different pollutants separately (**Figure 16b**). PCHs detected more types of metal ions than FHs did, and compound RBPCHs (C-RBPCHs) and MIPCHs showed extremely high detection sensitivities for metal ions. These disparities come from the abundance of metal chelators, the fact that even an extremely small amount of chelation causes obvious changes in hydrogel properties, and the advantages of molecular (ionic) imprinting technologies. Since metal ions can directly quench the fluorescence of some fluorophores, FHs for metal ion detection are easy to construct. However, these FHs lack specificity, and their detection sensitivities are relatively low. Therefore, they are mainly used as the indicator of heavy metals adsorbent materials. Compared to cations (metal ions), FHs can detect even more anions. As anions are electron-deficient groups, they can directly induce electron transfer and affect the electronic arrangement of fluorophores. These phenomena affect the fluorescence properties, particularly those of fluorophores. Therefore, CFHs also have the highest sensitivity for anion detection.

Considering their potential hazards, complex organic compounds, such as antibiotics, pesticides, and poisons, require high-precision linear quantitative detection. Therefore, researchers prefer to use FHs to detect them. However at present, FHs are not as sensitive as IOPCHs, MIPCHs, and biomolecule RBPCHs (B-RBPCHs) for these complex organic compounds. As for small organic molecules, they directly react with the functionalized hydrogel matrixes of PCHs, affecting their diffraction wavelengths; this is a simple detection strategy. However, FHs (and particularly the emerging GQDFHs) had far stronger detection sensitivities for small organic compounds than PCHs. The extremely rich organic groups of GQDs play an essential role in the detection of small molecular organics by GQDFHs. Gas molecules can replace the medium in the pores of hydrogel matrixes, directly changing the refractive index of PCHs; thus, the vast majority of OHs that can detect gas molecules are PCHs. However, the detection sensitivities of OHs to gas molecules need further improvement.

In microbiological detection, FHs were not used as the main body of detection but assisted other detection methods, such as RT-LAMP and PCR. This special mechanism allows FHs to detect more kinds of microorganisms than PCHs^[125-128], and BFHs also have high sensitivities for microbiological detection. Furthermore, molecular imprinting technologies can create highly specific cavities using microorganisms as templates; thus, MIPCHs also exhibit high sensitivities for microorganisms. As there were no LODs reported for environmental parameters, we plotted the frequencies of detection instead of LODs in the heatmap for environmental pollutant-detecting OHs (**Figure 16b**). Owing to the direct environmental stimuli-responsiveness of hydrogels, DRPCHs are undoubtedly the most suitable OHs for environmental pollutant detection.

5.2 Cross-relationships of different OHs

FHs and PCHs are two different development directions of OHs. They are not in competition but complement

each other. In the future, PCHs need to be faster and more sensitive to identify more environmental pollutants through visual detection. FHs need to accurately quantify more environmental pollutants through more portable fluorescent devices. Figure 17 presents the relationships between the different kinds of OHs. Although some PCHs (DRPCHs) can detect certain pollutants without target recognition modules, they cannot achieve high sensitivities. Improving the sensitivity of PCHs for complex macromolecules and even organisms requires combining molecular imprinting technologies and biological macromolecules. It is also necessary to use inverse opal structures to improve the sensitivity of signal expression.

Additionally, to improve the detection accuracy of PCHs, multiple PCHs can be combined. For example, two or more environmental stimuli-responsive hydrogels can be used to construct joint inverse opal structures^[43,79] and compounds^[82] or biomacromolecule^[63,68] receptors can be added to molecular imprinting cavities. This synergy can also be applied to FHs, for example, by combining QDs and compounds^[107,186] or simultaneously doping CDs and other QDs to form a double fluorescence system^[134]. In particular, all BFHs require the assistance of QDs or fluorophores, as no biomacromolecule emits fluorescence (except for the green fluorescent protein in luminescent microorganisms). Furthermore, some recent reports fused PCHs and FHs into a system called fluorescent PCHs^[159,160]. This may be an interesting new development direction, but more research is needed to determine whether the effects of the change in grating diffraction and SPR on fluorescence are beneficial.

6. Concluding remarks

Although OHs are mostly used in biological and medical fields, they have extensive application and development scope in environmental pollutant detection. Research and development of OHs may make detection of environmental pollutants more convenient, inexpensive, and efficient. It is also one of the ways to achieve in situ detection and online monitoring of the environment.

Herein, more than 60% of the examples of OHs were FHs, and only 30% were PCHs. The main advantage of FHs is the rapid quantitative on-site detection of pollutants as these sensitive fluorescence-based devices are small, portable, and inexpensive. Further, the fluorescence intensity of well-designed FHs can change linearly with varying pollutant concentration and the pollutant type can change the fluorescence wavelength, enabling the recognition and quantification of different pollutants. The detection sensitivities of some FHs even exceed those obtained using traditional methods. Therefore, they may become one of the most important research directions for OHs. QDFHs are one of the most promising classes of FHs because QDs exhibit bright fluorescence, photostability, excellent multiplexing ability, and controllable emission wavelength based on crystal size and material properties. More importantly, QDs are one of the best commercialized high-performance fluorophores^[224,225], affording the developed QDFHs high potential for inexpensive and large-scale production. However, owing to their potential environmental risks, heavy metal-based QDs are not suitable for environmental pollutant detection. By contrast, CDFHs may become mainstream in environmental pollutant detection owing to the wide sources and environmental friendliness of CDs^[145,146]. Notably, CDs can be simultaneously synthesized with hydrogel matrixes while preparing CDFHs^[158,159], which not only reduces the sensor fabrication cost and difficulty but also improves the stability and uniformity of fluorescence. FHs using GQDs as fluorophores have been reported since 2021^[178-181]. GQDFHs have shown extremely high detection sensitivities to pollutants, some even far surpassing those of traditional detection methods. As extremely complex polycyclic aromatic hydrocarbon molecular groups^[174], the properties of GQDs are more controllable and scalable than those of ordinary CDs. Hence, GQDFHs may be one of the most promising directions in environmental pollutant detection, although their cost remains high.

Although there are fewer reports on PCHs than FHs, PCHs are easily turned into visual detection kits and can rapidly and directly identify pollutants through changes in apparent color. Recently, rapid target recognition kits based on visual detection technologies have attracted increasing attention as they do not require any detection equipment or professional operators. The most salient example is the widespread application of COVID-19 antigen kits worldwide during the pandemic. Hence, PCHs hold great promise for inexpensive, rapid batch in situ detection in emergency cases. For FHs, the density, uniformity, coordination, and complex signal transmission paths of their internal fluorescence and target recognition units may affect detection

sensitivity. We think that applying supramolecular nanohydrogels, which have been widely studied in drug delivery systems^[226,227], to FHs could solve this problem. A single fluorescence unit, target recognition unit, and signal transmission and conversion unit are formed into a microscopic system and packaged in a nanohydrogel container. After multiple microscopic systems are encapsulated and form complete FHs, the density and uniformity of the fluorescence and acceptor units are guaranteed, and the microsystems do not interfere with each other. Thus, this system may improve the sensitivity of FHs.

Finally, almost all OHs can only be applied to detect one pollutant or several with similar properties. Therefore, an interesting OH-based sensor or detection kit development direction would be to integrate multiple OHs for different pollutant detection into a single sensor array to simultaneously detect multiple common or harmful environmental pollutants. We hope that this review will spark new ideas for the further application and development of OHs in the field of environmental pollutant detection.

Acknowledgements

The research was supported by the China National Natural Science Foundation (No. 22122601; 92043301; 91843301), and the Science and Technology Commission of Shanghai Municipality (20ZR1404300 and 212307128).

Tables

Table 1. Abbreviations

Abbreviation	Annotation	Abbreviation	Annotation
AAM	acrylamide	IFE	inner filter effect
ATAC	3-arylamidopropyl-trimethylammonium chloride	MIPCHs	molecular imprinted polymer hydrogels
AChE	acetylcholinesterase	MR-HT	morin and hydroxytryptamine
AAc	acrylic acid	MAA	methacrylic acid
APG	5'-O-acryloyl-2',3'-O-isopropylidene guanosine	NCs	nanoclusters
BisAA	<i>N,N'</i> -methylene acrylamide	NCFHs	nanocluster fluorescent hydrogels
BODIPY	boron-dipyrromethene	NIPAM	<i>N</i> -isopropylacrylamide
BTHPA	<i>N</i> -(3-(benzo[d]thiazol-2-yl)-4-hydroxyphenyl)acetamide	OHs	optical hydrogels
BuChE	butyrylcholinesterase	PS	polystyrene
BTBPA	<i>N</i> -(3-(benzo[d]thiazol-2-yl)-4(tertbutyldiphenylsilyloxy)phenyl)acetamide	PAM	polyacrylamide
BFHs	biomacromolecule fluorophore hydrogels	PBGs	photonic bandgap hydrogels
BLHs	bioluminescence hydrogels	PET	photoinduced crosslinking
B-RBPCBs	biomacromolecule receptor-bound photonic crystal hydrogels	PCR	polymerase chain reaction
CIP	ciprofloxacin	PEI	polyethyleneimine
CFHs	compound fluorophore hydrogels	PCHs	photonic crystal hydrogels
CDs	carbon dots	PVA	poly(vinyl alcohol)
CDFHs	carbon dot fluorophore hydrogels	PU	polyurethane
CdQDs	Cd-based quantum dots	PT-DNA	polythymidine
C-RBPCBs	compound receptor-bound photonic crystal hydrogels	QDs	quantum dots
Cu-atda	copper coordination polymer	QDFHs	quantum dot fluorescent hydrogels
CNFs	cellulose nanofibrils	RBPCBs	receptor-bound photonic crystal hydrogels
DRPCHs	directly responsive photonic crystal hydrogels	RT-LAMP	reverse transcription loop-mediated isothermal amplification
dsDNA	double-stranded DNA	RCA	rolling circle amplification
ESIPT	excited-state intramolecular proton transfer	ssDNA	single-stranded DNA
FHs	fluorescent hydrogels	SiQDs	silicon quantum dots
FRET	fluorescence resonance energy transfer	SPR	surface plasmon resonance
GAM	glycidyl methacrylate	SA	sodium alginate
GQDs	graphene quantum dots	SD	salicylaldehyde
GQDFHs	graphene quantum dot fluorescent hydrogels	TB	thiosemicarbazide
GPTs	glycated proteins	TEMED	<i>N,N,N,N</i> -tetramethylethylenediamine

Abbreviation	Annotation	Abbreviation	Annotation
HEMA	2-hydroxyethyl methacrylate	TMB	3,3',5,5'-tetra
IOPCHs	inverse opal-structured photonic crystal hydrogels	8-HQ	8-hydroxyqu
ICT	intramolecular charge transfer		

Table 2. Properties and chemical construction of several typical hydrogel monomers used to construct different optical hydrogels

	Hydrogel monomer property	Hydrogel monomer property	Hydrogel monomer property	Hydrogel monomer	Abbreviation	Chemical formula	
	Property I	Property II	Property III				
Photonic crystals hydrogels	Swelling Nanometer pore Static electricity contraction	Hygroscopicity	-	Acrylamide glycol	AGI		
				Methylation Ionic liquid reaction	Acrylamide	AAM	
			pH responsiveness	-	2-Hydroxyethyl methacrylate	HEMA	
				-	<i>N,N,N,N</i> -Tetraethyl ethylenediamine	TEMED	
			Temperature responsiveness	-	Acrylic acid	AAc	
				-	<i>N</i> -isopropylacrylamide	NIPAm	
				-	<i>N, N'</i> -methylene acrylamide	BisAA	
			Metal ion complexation	-	3-Arylamidopropyl-trimethylammonium chloride	ATAC	
				-	Pentaethylenehexa	PEHA	
				-	Vinyl alcohol	PVA	
		-	Polystyrene	PS			
		-	Methacrylic acid	MAA			

	Hydrogel monomer property	Hydrogel monomer property	Hydrogel monomer property	Hydrogel monomer	Abbreviation	Chemical formula
Fluorescent hydrogels	3D porous frameworks Dispersing acceptor Leakage prevention Antipollution Target adsorption Dispersing acceptor	Biocompatibility	Grafting	Oxidized agarose	-	-
			Abundant acceptor sites	Sodium alginate	SA	
		Capture and ionize gas Fluorescence		Polyurethane	PU	
				<i>N</i> -(3-(benzo[d]thiazol-2-yl)-4-(tertbutyldiphenylsilyloxy)phenyl)acetamide	BTBPA	
		Metal ion complexation		Chitosan	-	-
				Polythioctic acid Carbonate	PTA-	
		Synchronous preparation with Quantum dot properties	Silica aerogel	SiO ₂ hydrogel		

Table 3. Inverse opal-structured photonic crystal hydrogels for detecting different kinds of chemical molecules

Target type	Target	Template	Hydrogel monomer	Crosslinker	Receptor	Detection mode	LOD/Accuracy	Ref.
Microorganism	<i>Candida albicans</i> Gram-negative bacterium	PS	Con A	Glutaral	Con A	Debye diffraction	32 CFU·mL ⁻¹	[67]
			GPTs	Glutaral	GPTs	Bragg diffraction	58 CFU·mL ⁻¹	[68]

Target type	Target	Template	Hydrogel monomer	Crosslinker	Receptor	Detection mode	LOD/Accuracy	Ref.
	Rotavirus	SiO ₂	NIPAm & AAc	BisAA	Protein A & monoclonal rotavirus antibody		1.27 mg·mL ⁻¹	[44]
Antibiotic	Glycine	PS	AAM & AAc	BisAA	Tetracycline & Cu(II)	Bragg diffraction	10 ⁻¹⁰ M	[69]
	Sarin		DEAP & AAm & AG501	BisAA	BuChE		10 ⁻¹⁵ M	[64]
	Imidacloprid	SiO ₂	MAA & EGDMA	AIBN	-		10 ⁻⁵ g·L ⁻¹	[86]
	Tetracycline	PS	AAM & EDMA	AIBN	-		0.05 µg·kg ⁻¹	[84]
	Ciprofloxacin		AAM & AAc	BisAA	Tryptophan & Zn(II)		10 ⁻¹⁰ M	[70]
	Penicillin		AAM & AAc	BisAA	Penicillinase	Debye diffraction	1 µM	[63]
Micromolecule	SCN ⁻	PS & PNIPAM	PEG-2000 & IPDI & BDO @ NIPAM	BisAA	Water	Bragg diffraction	5 µM	[79]
	Multi-solvents	PS & AAc	TiO ₂ @ AAM & PEGDA & AMPS	BisAA	-		-	[75]
	H ₂ O ₂	PS	HRP & BSA	Glutaral	HRP		8.8 × 10 ⁻⁶ M	[76]
Gas molecule	CO ₂	SiO ₂	DMAPMA	BisAA	Amidogen	Bragg diffraction	0.2 vol%	[62]
	Alcohols, acetone	MMA	MMA & CMC	AAM	-		110 ppm 102 ppm	[78]
	H ₂ O ₂	PS & SiO ₂	MMA & VBC	AIBN	-		0.51 g·L ⁻¹	[77]
	<i>o</i> -xylene						0.41 g*L ⁻¹	
	<i>m</i> -xylene						0.17 g*L ⁻¹	
	<i>p</i> -xylene							
Heavy metal	Be ²⁺	PS	AAM	BisAA	Benzo-9-crown-3	Bragg diffraction	10 ⁻¹¹ M	[59]

Target type	Target	Template	Hydrogel monomer	Crosslinker	Receptor	Detection mode	LOD/Accuracy	Ref.
	Cd ²⁺		AAm	BisAA	1-allyl-2-thiourea		0.01 mM	[55]
Environmental parameters	Temperature	PS	NIPAM & AAc	TEMED	-	Bragg diffraction	0.01 °C (Accuracy)	[44]
	pH	SiO ₂	EDMA & AAc	Irgacure-651	-		0.01 (Accuracy)	[43]

Note: - indicates that there are no relevant contents or description, and @ represents a double-layer structure. LOD: limit of detection; PS: polystyrene spheres; DEAP: 2,2-diethoxyacetophenone; AG501: resin type; EGDMA: ethylene glycol dimethylacrylate; AIBN: azobisisobutyronitrile; PEG-2000: polyethylene glycol 2000; IPDI: isophorone diisocyanate; BDO: 1,4-butanediol; AMPS: 2-acrylamido-2-methyl-propanesulfonic acid; DMAPMA: dimethyl aminopropyl methacrylamide; MMA: methyl methacrylate; CMC: sodium carboxymethyl cellulose; VBC: 4-vinylbenzyl chloride. The full forms of the remaining abbreviations can be found in the text or Table 1.

Table 4. Introduction to the principles of fluorescence emission and quenching

Principle	Description	Graphical description	Graphical description
Photoinduced electron transfer (PET)	Fluorophores (F) and acceptors (A) are linked by a chemical rigid bridge (B) to form an F-B-A system. Normally, excitation light causes electron transfer from A to F and inhibits fluorescence. When the target interacts with A, electron transfer is inhibited or suppressed, allowing the fluorescence of F recovers. ^[94]	Ground state	Excited by targets

Principle	Description	Graphical description	Graphical description
Intramolecular charge transfer (ICT)	Fluorophores are in direct contact with acceptors, allowing orbital overlap. One end of the molecule is electron-rich and the other is electron-poor. Normally, this tendency is exacerbated by excitation light, generating numerous dipoles. When the target interacts with the acceptor, the excited state dipoles are repelled (blue shift) or attracted (red shift). ^[95]		
Excited-state intramolecular proton transfer (ESIPT)	Irradiation by excitation light puts the fluorophore in the excited state, inducing proton transfer between the proton donors and proton acceptors inside the molecule, forming tautomers with different fluorescence properties. ^[96]		
Fluorescence resonance energy transfer (FRET)	Fluorophore contains a fluorescence donor (FD) and fluorescence acceptor (FA). Interaction with the target induces energy transfer from FD to FA via nonradiative dipole–dipole coupling under the action of excitation light, inducing fluorescence of FA. ^[97]		

Principle	Description	Graphical description	Graphical description
Excimer/excimer	An excited-state fluorophore forms a complex with the same ground-state fluorophore (excimer) or different ground-state fluorophore (excimer). When the excimer/excimer interacts with the target, double fluorescence of the excited-state fluorophore and excimer/excimer can be observed. ^[98]		

Table 5. Limit of detection (LOD) of different pollutants in their corresponding reference test standards

Contaminants	LOD	Method	Reference standards
Pb ²⁺	0.2 µg·L ⁻¹	Atomic Absorption Spectroscopy	GB 7475-1987
Cr ⁶⁺	1 µg·L ⁻¹	Ion Chromatography	ASTM D5257-17
Hg ²⁺	0.05 µg·L ⁻¹	Atomic Absorption Spectroscopy	ISO 12846:2012
Sr ²⁺	13 µg·L ⁻¹	Atomic Absorption Spectroscopy	ASTM D3920-18
Fe ³⁺	100 µg·L ⁻¹	Atomic Absorption Spectroscopy	GB 11911-1989
Cu ²⁺	1 µg·L ⁻¹	Atomic Absorption Spectroscopy	GB 7475-1987
Al ³⁺	5 mg·L ⁻¹	Atomic Absorption Spectroscopy	ISO 12020:1997
Cd ²⁺	0.3 µg·L ⁻¹	Atomic Absorption Spectroscopy	DIN EN ISO 5961:1995
Be ²⁺	33.5 µg·L ⁻¹	Atomic Absorption Spectroscopy	ASTM D4382-18
Ni ²⁺	50 µg·L ⁻¹	Atomic Absorption Spectroscopy	GB 11912-1989
ClO ⁻	1 µg·L ⁻¹	Titrimetry	GB19106-2003
SCN ⁻	5 µg·L ⁻¹	Flow injection analysis	ISO 20950-1:2018
HPO ₄ ²⁻	100 µg·L ⁻¹	Capillary ion electrophoresis	ASTM D6508-15
H ₂ PO ₄ ⁻	100 µg·L ⁻¹	Capillary ion electrophoresis	ASTM D6508-15
F ⁻	50 µg·L ⁻¹	Capillary ion electrophoresis	ASTM D6508-15
CrO ₄ ²⁻	1 µg·L ⁻¹	Ion chromatography	ASTM D5257-17
NO ₂ ⁻	50 µg·L ⁻¹	Nitrate reductase	ASTM D7781-14
Tetracycline	50 µg·L ⁻¹	HPLC	GB 18932.4-2002
Ochratoxin	0.1 µg·L ⁻¹	HPLC	ONORM EN 14133:2009
Penicillin	6 µg·L ⁻¹	HPLC	GB5009.185-2016
Augmentin	1 µg·L ⁻¹	HPLC	GB5009.185-2016
Rifampicin	3 µg·L ⁻¹	-	The average of the reporting methods
Nitrofurantoin	0.5 µg·L ⁻¹	HPLC-MS	BG/T 21311-2007
Lincomycin	15 µg·L ⁻¹	GC-MS	GB 29685-2013
Oxytetracycline	5 µg·L ⁻¹	HPLC-UV	BG/T 20764-2006
Doxycycline	10 µg·L ⁻¹	HPLC	BG/T 18932.4-2002
Aflatoxin	0.1 µg·L ⁻¹	HPLC	DS/EN ISO14501:2021

Contaminants	LOD	Method	Reference standards
Ciprofloxacin	1 $\mu\text{g}\cdot\text{L}^{-1}$	HPLC-MS	BG/T 22985-2008
Kanamycin	5 $\mu\text{g}\cdot\text{L}^{-1}$	HPLC-MS	GB/T 22969-2008
Cypermethrin	18.6 $\mu\text{g}\cdot\text{L}^{-1}$	GC	GB 9565-1988
Organophosphorus	1 $\mu\text{g}\cdot\text{L}^{-1}$	GC	BS EN 12918:1999
Dichlorvos	0.05 $\mu\text{g}\cdot\text{L}^{-1}$	GC	GB 13192-1991
Imidacloprid	20 $\mu\text{g}\cdot\text{L}^{-1}$	HPLC	GB/T 23379-2009
Paraoxon	0.05 $\mu\text{g}\cdot\text{L}^{-1}$	GC	GB 13192-1991
Carbamate	0.1 $\mu\text{g}\cdot\text{L}^{-1}$	UPLC-TQMS	HJ-827-2017
Sarin	0.0046 $\mu\text{g}\cdot\text{L}^{-1}$	GC	GJB 3665-1999
PFOS	0.02 $\mu\text{g}\cdot\text{L}^{-1}$	HPLC-MS	GB 5009.253-2016
Amino acid	0.13 $\mu\text{g}\cdot\text{L}^{-1}$	Ion-exchange chromatography	GB 5009.124-2016
Phenol	0.1 $\mu\text{g}\cdot\text{L}^{-1}$	GC-MS	ISO 18857-1:2005
NH ₃	200 $\mu\text{g}\cdot\text{L}^{-1}$	Potentiometric	ISO 6778:1984
<i>o</i> -Xylene	5 $\mu\text{g}\cdot\text{L}^{-1}$	GC	GB 11890-1989
<i>m</i> -Xylene	5 $\mu\text{g}\cdot\text{L}^{-1}$	GC	GB 11890-1989
<i>p</i> -Xylene	5 $\mu\text{g}\cdot\text{L}^{-1}$	GC	GB 11890-1989
Formaldehyde	50 $\mu\text{g}\cdot\text{L}^{-1}$	Spectrophotometry	GB 13197-1991
H5N1	4 HAU	Antibody detection	GB T 27535-2011
<i>E. coli</i>	15 CFU	Coliform bacteria count	GB 4789.3-2016
H ₂ O ₂	0.6 $\times 10^{-6}$ M	Peroxidase enzyme fluorescence	ASTM D6363-20
H ₂ S	1 ppb/v	Rate of change of reflectance	ASTM D4323-21
Methanol gas	5 $\text{mg}\cdot\text{m}^{-3}$	GC	GBT 16062-1995
Ethanol gas	5 $\text{mg}\cdot\text{m}^{-3}$	GC	GBT 16062-1995
CO ₂	0.0001	Non-spectral infrared gas analysis	GBT 18204.24-2000

Illustrate: When there are several different detection standards for the same substance, the standard with the lowest detection limit was selected. For pollutants without a detection limit in the corresponding detection standards or if the corresponding detection standards could not be found, their normalized values were recorded as 1 when the sensitivities were calculated (*Figure 7c*), indicating that this type of contamination could be detected and the default detection limit was equivalent to that of normal detection methods. As there were no LODs reported for environmental parameters, we plotted the frequencies of detection instead of LODs in the heatmap in *Figure 7c* for environmental pollutant-detecting OHs.

Figures

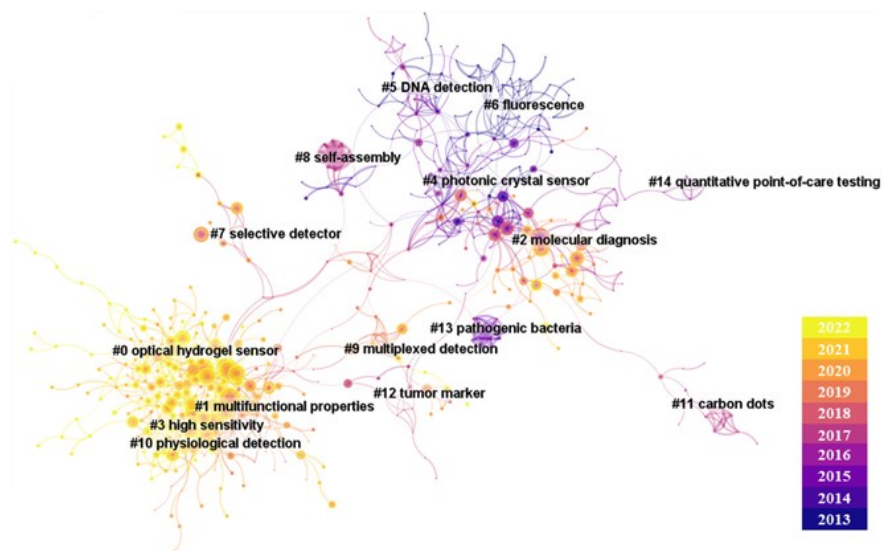


Figure 1. Research trend analysis of optical hydrogel detection technologies based on CiteSpace 6.1. All data came from the 1000 most relevant documents on the Web of Science Core Collection in the past 10 years, and the extracted contents include the title, keywords, abstract, and references of papers. The nodes represent keywords, the size of nodes indicates the frequency of the keyword in the journal, and the connection between the nodes represents the interconnection between the keywords. The keywords with the highest frequency show in the form of tags. The smaller the serial number, the higher the frequency, and #0 is the search keyword.

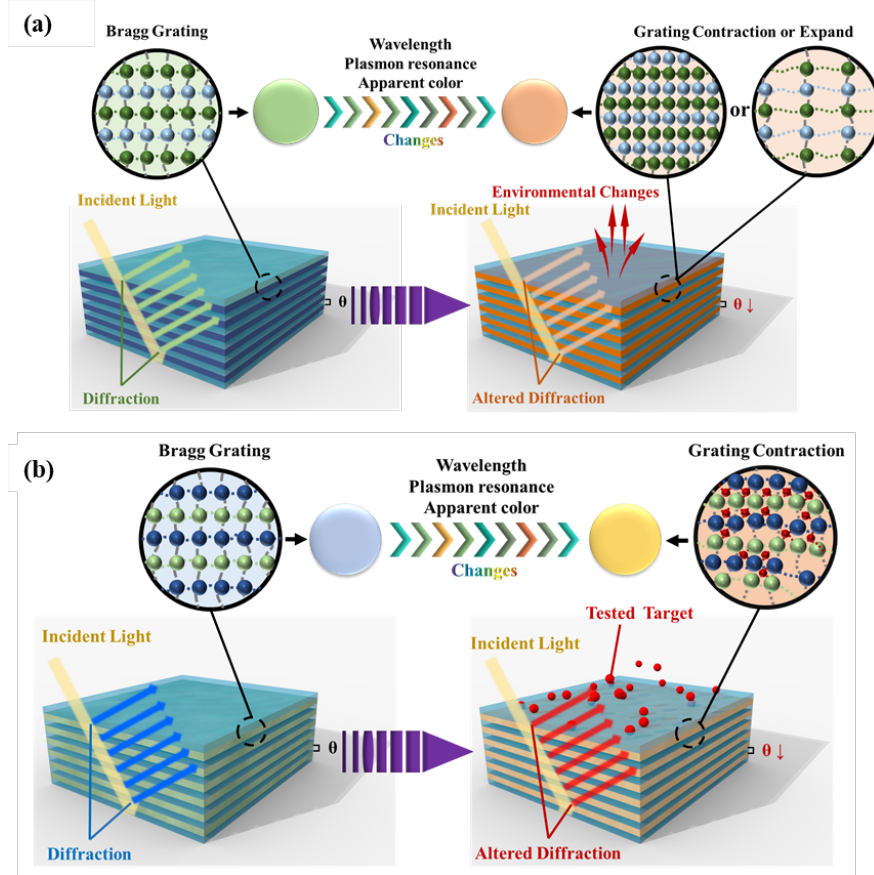


Figure 2. Schematic diagrams of photonic crystal hydrogel sensors. (a) Environmental stimuli-responsive photonic crystal hydrogel sensors. (b) Photonic crystal hydrogel sensors combined with ions and receptors.

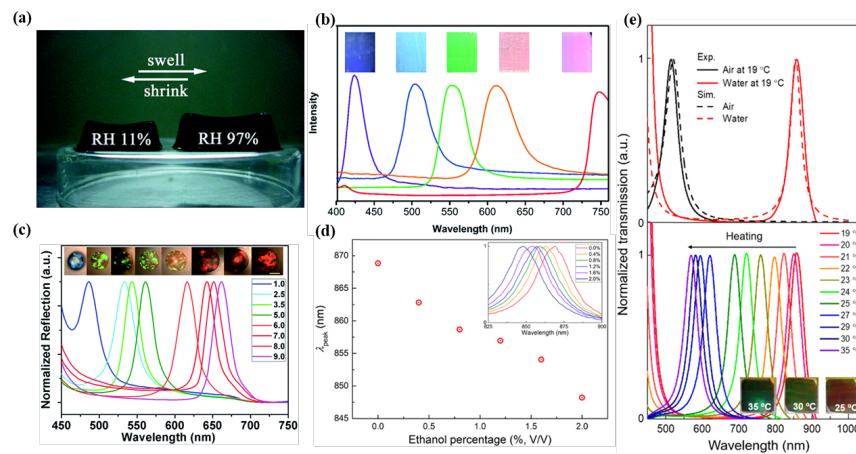


Figure 3. The response modes of directly responsive photonic crystals hydrogels to environmental parameters. (a) The matrices of directly responsive photonic crystals hydrogels shrinkage and expansion due to changes in environmental parameters (humidity)^[41]. Effects of apparent colors and reflectance spectrums of directly responsive photonic crystals hydrogels caused by changes in environmental parameters

((b)humidity^[42] and (c) pH values^[43]). Variations of the multistimuli-responsive optical hydrogel in resonance spectrum at (d) different ethanol concentrations and (e)temperatures^[46].

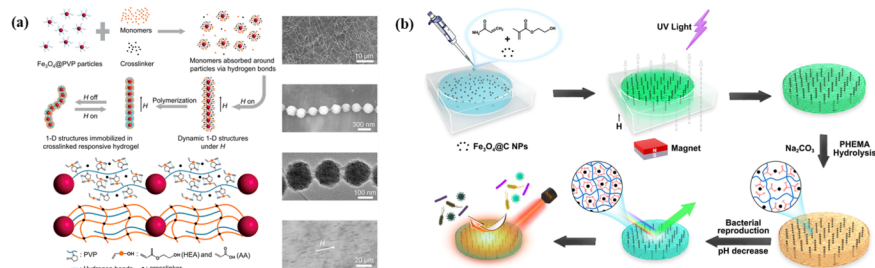


Figure 4. Mechanisms of two typical direct-response photonic crystal hydrogels. (a) Synthetic mechanism and characterization of submicron photonic crystals via the H-bond-guided template method, taking the synthesis of pH-responsive directly responsive photonic crystal hydrogels as an example^[47]. (b) Illustration of the fabrication and responsive mechanism of directly responsive photonic crystal hydrogels for bacterial diagnosis and disinfection^[48].

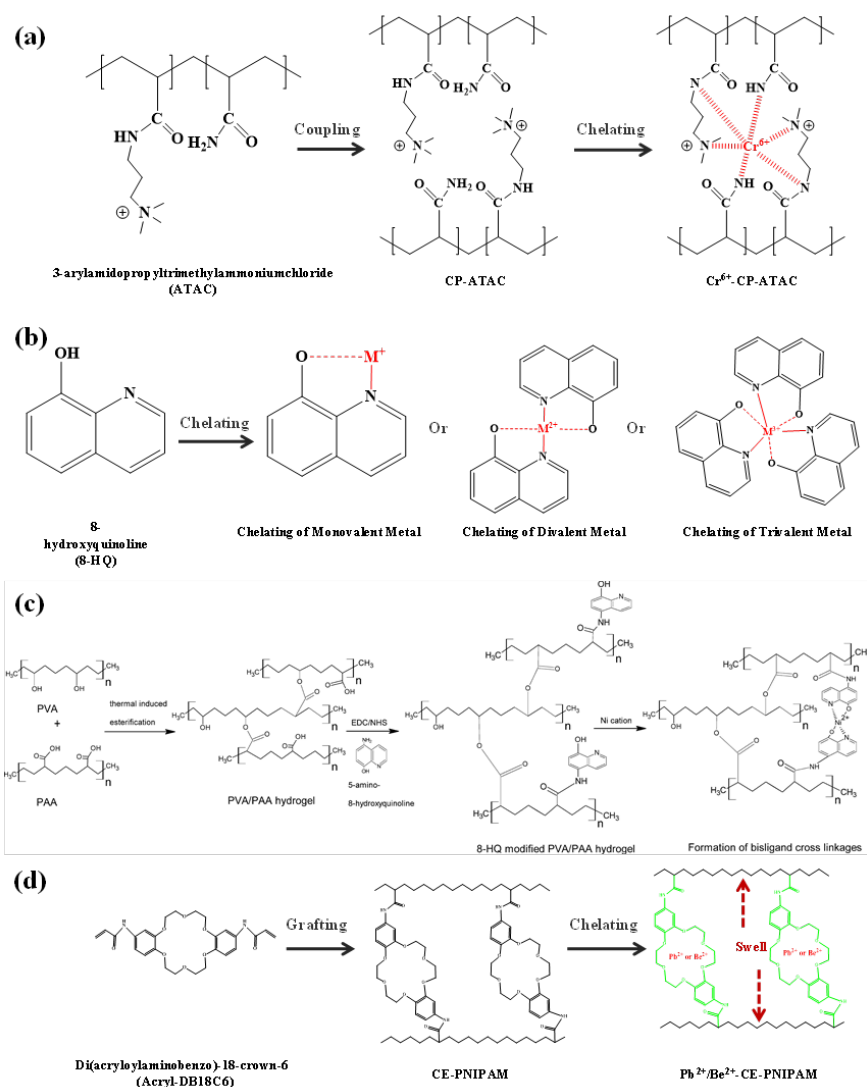


Figure 5. Recognition of heavy metals by compound receptors in photonic crystal hydrogels. **(a)** Molecular structure of CP-ATAC and chelation of Cr⁶⁺ in CP-ATAC. **(b)** Molecular structure of 8-HQ and chelation of different valence metals.**(c)** Grafting of 8-HQ on hydrogel monomers^[52]. **(d)** Introduction of crown ether groups, molecular structure of CE-PNIPAM, and chelation of Pb²⁺ and Be²⁺ in CE-PNIPAM.

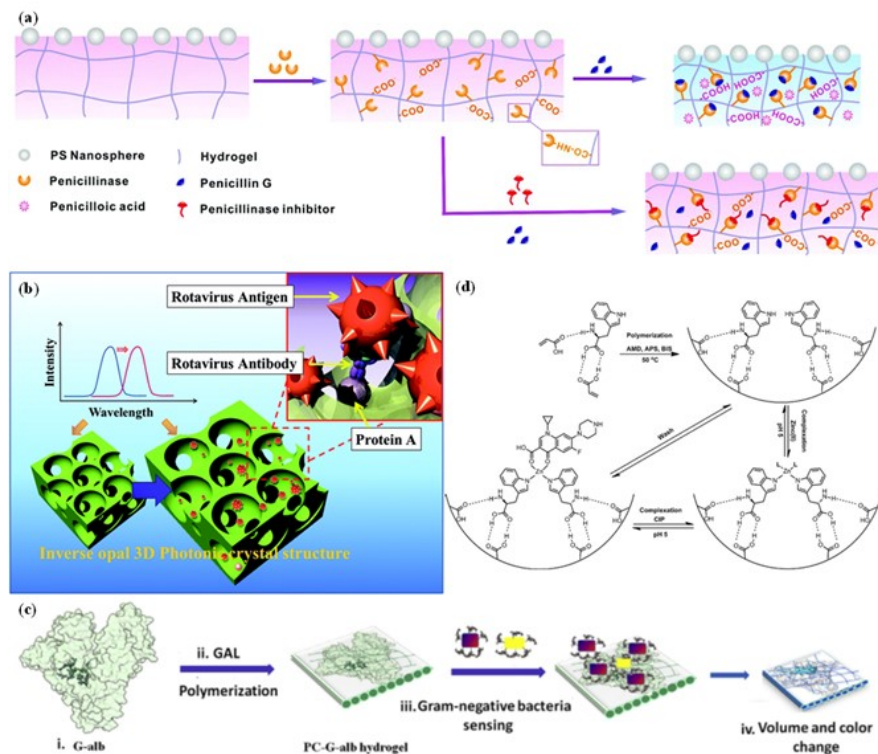


Figure 6. The operating principles of some special photonic crystal hydrogels. (a) Recognition and response strategies of photonic crystal hydrogels to penicillin G^[63]; (b) Working principle of a label-free virus sensor based on an inverse opal 3D Photonic crystal hydrogels^[65]; (c) Construction of photonic crystal hydrogels that can recognize *E. coli* by glycosylated proteins^[68]; (d) The construction mechanism of ternary complexes-based photonic crystal hydrogel sensors, and how it captures ciprofloxacin compounds^[70];

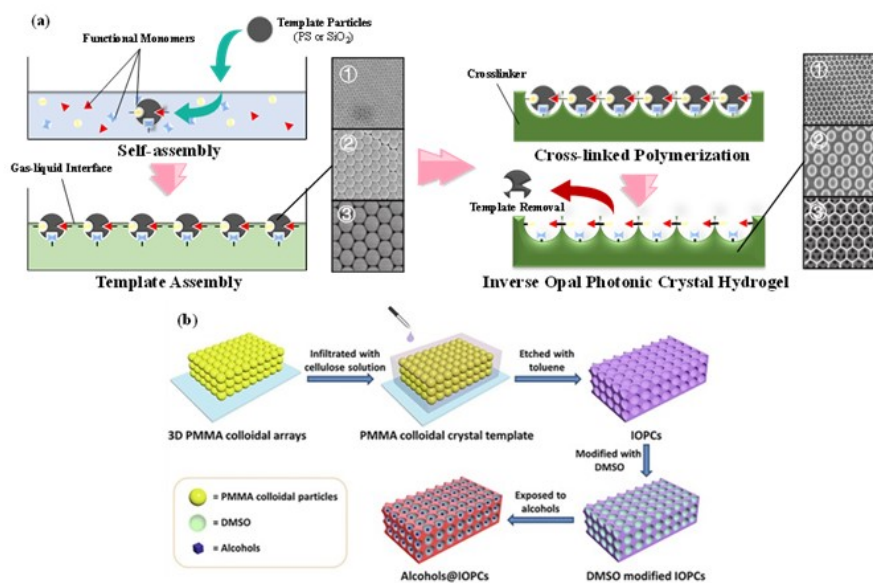


Figure 7. (a) Preparation process of inverse opal photonic crystal hydrogels. SEM images 1^[75], 2^[76], and 3^[77] from different literatures; (b) Construction of photonic crystal hydrogels that can identify gas targets based on anti-opal structures^[78].

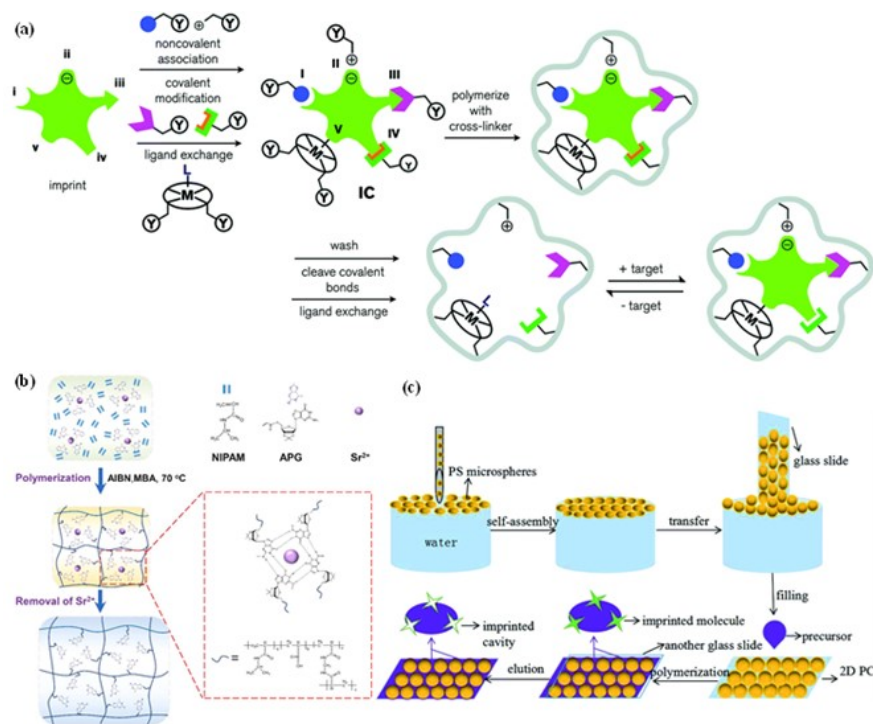


Figure 8. Constructive process of molecular imprinting based photonic crystals hydrogels (a) Five main types of molecular imprinting: (i) noncovalent, (ii) electrostatic/ionic, (iii) covalent, (iv) semicovalent, and (v) metal centre coordination^[81]; (b) The planar G-quartets formed in photonic crystals hydrogels using Sr²⁺ as templates^[82]; (c) Using tetracycline as the template molecules, specific imprints are engraved in photonic crystal hydrogels with anti-opal structures^[84].

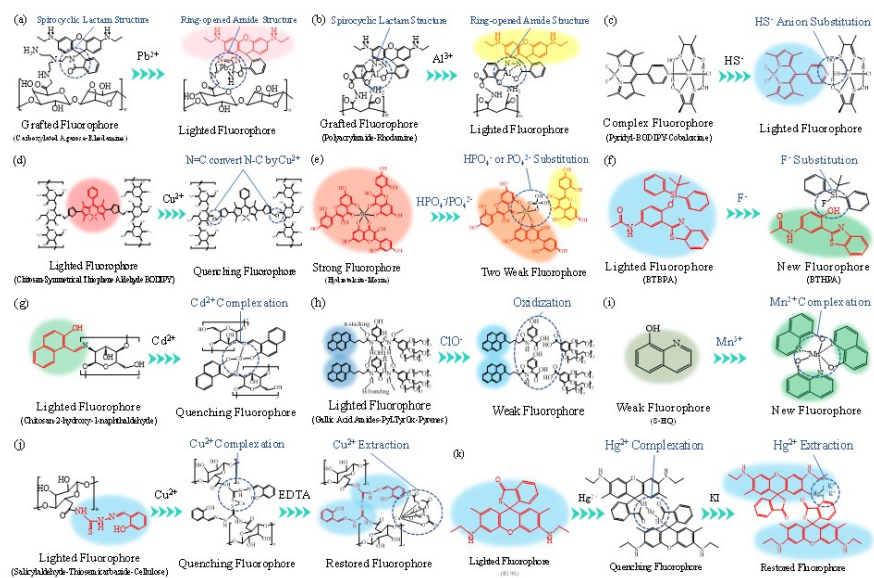


Figure 9. Response mechanisms of compound fluorophore hydrogels to targets. (a) Response of rhodamine to Pb^{2+} and (b) Al^{3+} . (c) Response of BODIPY derivatives to HS^- and (d) Cu^{2+} . (e) Response of morin to HPO_4^- or $H_2PO_4^-$. (f) Response of BTBPA to F^- . (g) Response of chitosan-2-hydroxy-1-naphthaldehyde to Cd^{2+} . (h) Response of gallic acid amides-PyL-Tyr-Ox-pyrenes to ClO^- . (i) Response of 8-HQ to Mn^{3+} . (j) Response of SD-TB to Cu^{2+} . (k) Response of R19S to Hg^{2+}

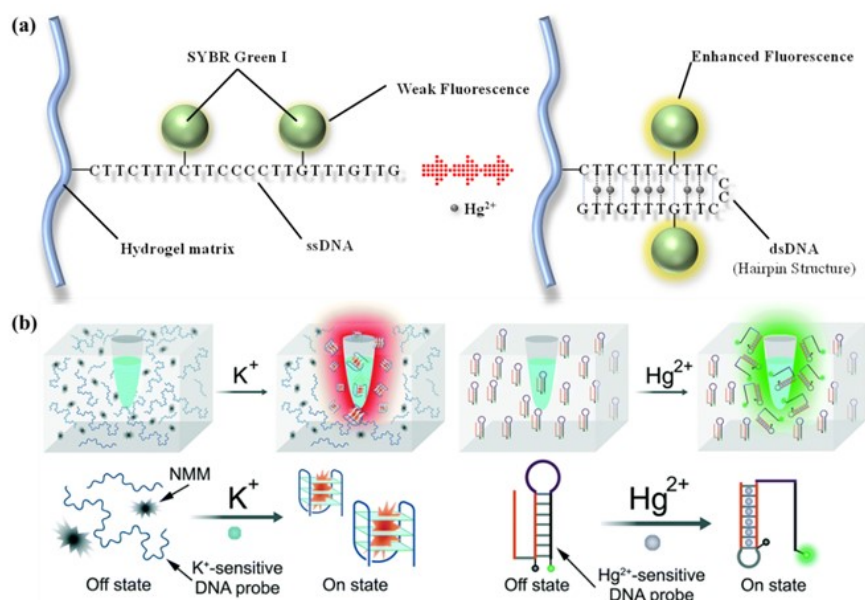


Figure 10. DNA-based fluorescent hydrogels that can detect heavy metals. (a) Under the guidance of Hg^{2+} , single-stranded DNA is folded into double-stranded DNA with a hairpin structure and further enhances the fluorescence of SYBR Green I; (b) The response principles of DNA-based fluorescent hydrogels to different metal ions^[115].

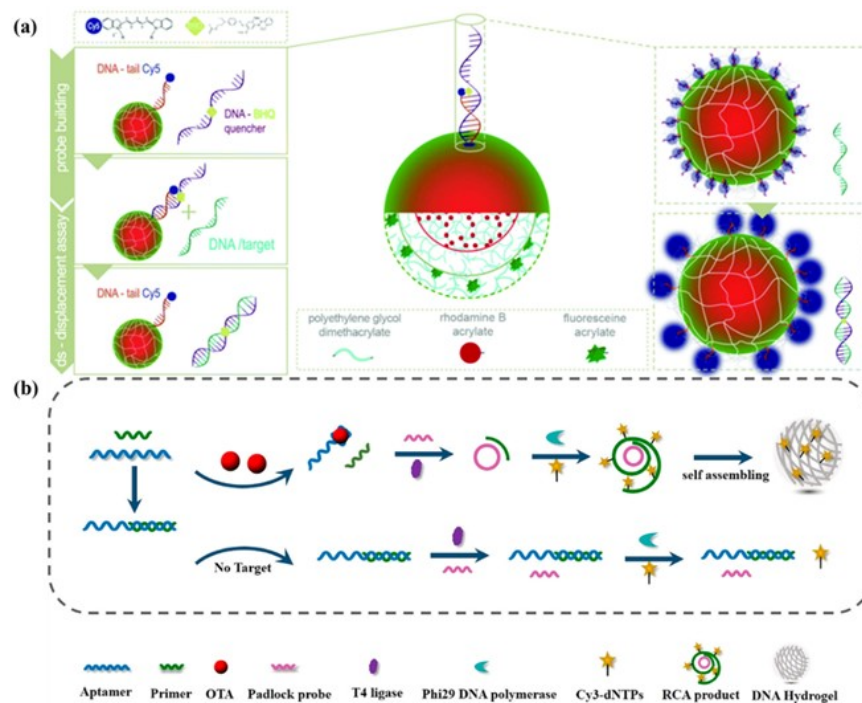


Figure 11. The operating principles of some special fluorescent hydrogels, which use DNA as the acceptor. (a) In the microgel particles, the target viral DNA hybridizes to quencher in the tail of single-stranded DNA and results in fluorescence recovery.^[122]; (b) Ochratoxin A binds to aptamers to initiate rolling circle amplification and induce fluorescence of Cy3dUTP^[129].

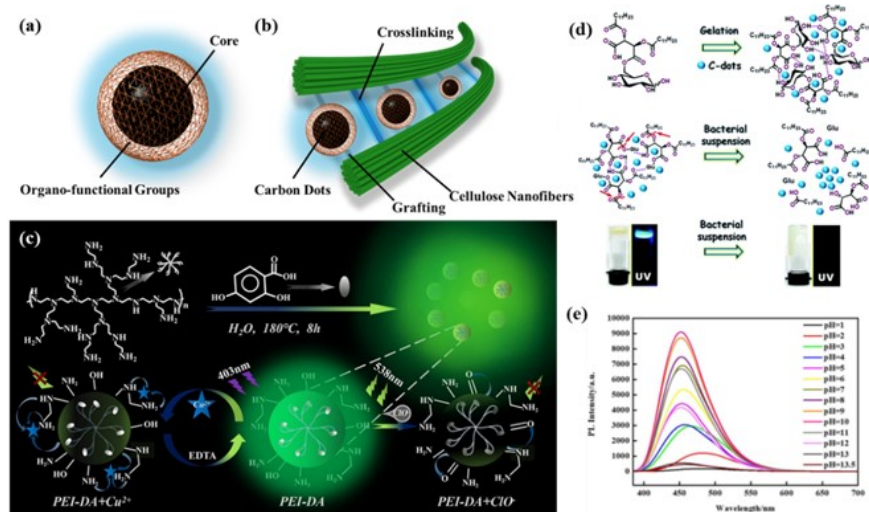


Figure 12. (a) Structure of fluorescent carbon dots; (b) Fluorescent carbon dots immobilized by cellulose nanofibers; (c) The fluorescence quenching of polyethyleneimine-doped carbon dot fluorescent hydrogels by ClO⁻^[162]; (d) Fluorescence of the enzyme-embedded carbon dot fluorescent hydrogels is quenched in by induction of bacteria^[169]. (e) The changes of photoluminescence spectate of two carbon dot fluorescent hydrogels with pH detection capability at different pH^[171].

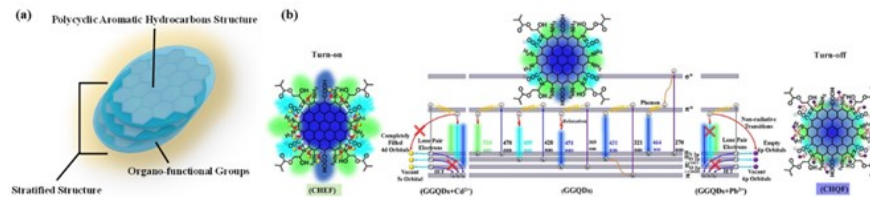


Figure 13. (a) Universal structure of fluorescent graphene quantum dots; (b) Sensing mechanisms of the glyceryl methacrylate-functionalized GQDs embedded fluorescent hydrogels to Cd²⁺ and Pb²⁺[178]

Hosted file

image41.emf available at <https://authorea.com/users/581749/articles/622191-application-of-optical-hydrogels-in-environmental-sensing>

Figure 14. Environmental sensing by the luminescent microorganisms embedded hydrogels. (a) The plasmids of Genetic recombination fluorescent microorganisms (GFPG: green fluorescent protein gene, ARG: antibiotics resistance gene, ORF: open reading frame); (b) Luminescent response of strains wrapped in hydrogel to 2,4-dinitotoluene in soil^[206], (c) Hydrogel microspheres immobilized with recombinant *E. coli* are used to detect heavy metals in water, each microsphere is wrapped in a tough semi-permeable hydrogel shell to prevent leakage of engineered bacteria^[18].

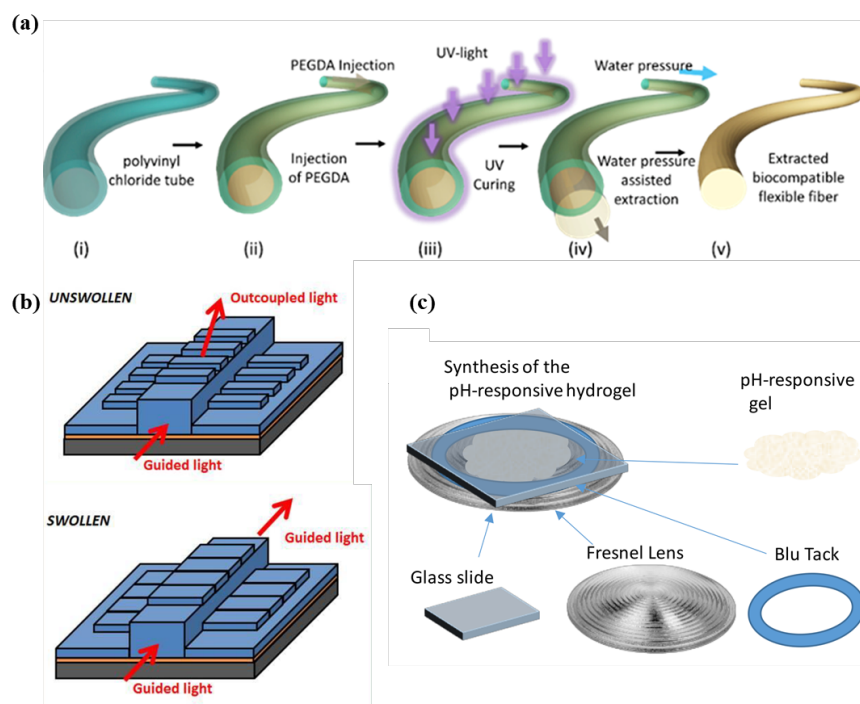


Figure 15. Three other types of optical hydrogel sensors.(a) Fiber-based optical hydrogel sensors^[213]; (b) Waveguide-based optical hydrogel sensors^[216]; (c) Fresnel lens-based optical hydrogel sensor^[219].

Hosted file

image43.emf available at <https://authorea.com/users/581749/articles/622191-application-of-optical-hydrogels-in-environmental-sensing>

Hosted file

image44.emf available at <https://authorea.com/users/581749/articles/622191-application-of-optical-hydrogels-in-environmental-sensing>

Figure 16. Statistical analysis of optical hydrogel research cases. **(a)** Sample numbers for different pollutants detected by fluorescent hydrogels and photonic crystal hydrogels (numbers on stacking columns represent identifiable target species). Number of samples: 114. **(b)** Detection sensitivities of different types of optical hydrogels for different contaminants (Note: 1.0 indicates that the sensitivity of this type of optical hydrogel is the same as that of the standard method; samples with sensitivity <1% that of the traditional method appear in pure black).

References

- [1] M. Mahmoudpour, J. Ezzati Nazhad Dolatabadi, M. Torbati, A. Homayouni-Rad, *Biosens. Bioelectron.* **2019** , *127* , 72.
- [2] H. Huang, J. U. Qureshi, S. Liu, Z. Sun, C. Zhang, H. Wang, *B. Environ. Contam. Tox.* **2020** , *107* , 754.
- [3] C. H. Voon, N. M. Yusop, S. M. Khor, *Talanta* **2022** , *241* , 123271.
- [4] H. Zhang, B. Li, Y. Liu, H. Chuan, Y. Liu, P. Xie, *J. Hazard. Mater.* **2022** , *424* , 127406.
- [5] W. Guo, C. Zhang, T. Ma, X. Liu, Z. Chen, S. Li, Y. Deng, *J. Nanobiotechnol.* **2021** , *19* .
- [6] X. Hou, L. Mu, F. Chen, X. Hu, *Environmental science. Nano* **2018** , *5* , 2216.
- [7] Y. Liu, G. Su, B. Zhang, G. Jiang, B. Yan, *Analyst (London)* **2011** , *136* , 872.
- [8] L. Shi, N. Li, D. Wang, M. Fan, S. Zhang, Z. Gong, *TrAC Trends in Analytical Chemistry* **2021** , *134* , 116131.
- [9] L. Zhang, D. Peng, R. Liang, J. Qiu, *TrAC Trends in Analytical Chemistry* **2018** , *102* , 280.
- [10] J. Liu, S. Qu, Z. Suo, W. Yang, *National Science Review* **2021** , *8* .
- [11] O. Wichterle, D. Lím, *Nature (London)* **1960** , *185* , 117.
- [12] G. An, F. Guo, X. Liu, Z. Wang, Y. Zhu, Y. Fan, C. Xuan, Y. Li, H. Wu, X. Shi, C. Mao, *Nat. Commun.* **2020** , *11* .
- [13] B. Ding, P. Zeng, Z. Huang, L. Dai, T. Lan, H. Xu, Y. Pan, Y. Luo, Q. Yu, H. Cheng, B. Liu, *Nat. Commun.* **2022** , *13* .
- [14] X. Duan, J. Yu, Y. Zhu, Z. Zheng, Q. Liao, Y. Xiao, Y. Li, Z. He, Y. Zhao, H. Wang, L. Qu, *Acs Nano* **2020** , *14* , 14929.
- [15] G. G. Giobbe, C. Crowley, C. Luni, S. Campinoti, M. Khedr, K. Kretzschmar, M. M. De Santis, E. Zambaiti, F. Michielin, L. Meran, Q. Hu, G. van Son, L. Urbani, A. Manfredi, M. Giomo, S. Eaton, D. Cacchiarelli, V. S. W. Li, H. Clevers, P. Bonfanti, N. Elvassore, P. De Coppi, *Nat. Commun.* **2019** , *10* .
- [16] H. Jin, G. Zhao, J. Hu, Q. Ren, K. Yang, C. Wan, A. Huang, P. Li, J. Feng, J. Chen, Z. Zou, *Acs Appl. Mater. Inter.* **2017** , *9* , 25755.
- [17] S. Park, H. Yuk, R. Zhao, Y. S. Yim, E. W. Woldegebriel, J. Kang, A. Canales, Y. Fink, G. B. Choi, X. Zhao, P. Anikeeva, *Nat. Commun.* **2021** , *12* .
- [18] T. Tang, E. Tham, X. Liu, K. Yehl, A. J. Rovner, H. Yuk, C. de la Fuente-Nunez, F. J. Isaacs, X. Zhao, T. K. Lu, *Nat. Chem. Biol.* **2021** , *17* , 724.
- [19] J. Wang, T. Lu, M. Yang, D. Sun, Y. Xia, T. Wang, *Sci Adv* **2019** , *5* , u8769.

- [20] L. Cui, Y. Yao, E. K. F. Yim, *APL Bioengineering* **2021** , 5 , 31509.
- [21] N. Zoratto, P. Matricardi, *Adv. Exp. Med. Biol.* **2018** , 1059 , 155.
- [22] M. Hamidi, A. Azadi, P. Rafiei, *Adv. Drug Deliver. Rev.* **2008** , 60 , 1638.
- [23] X. Hu, Z. Xia, K. Cai, *Journal of materials chemistry. B, Materials for biology and medicine* **2022** , 1 , 1157.
- [24] F. Mo, K. Jiang, D. Zhao, Y. Wang, J. Song, W. Tan, *Adv. Drug Deliver. Rev.* **2021** , 168 , 79.
- [25] Z. Zhang, W. Jiang, X. Xie, H. Liang, H. Chen, K. Chen, Y. Zhang, W. Xu, M. Chen, *ChemistrySelect* **2021** , 6 , 12358.
- [26] J. Y. C. Lim, S. S. Goh, X. J. Loh, *ACS Materials Letters* **2020** , 2 , 918.
- [27] S. Khosravimelal, M. Mobaraki, S. Eftekhari, M. Ahearne, A. M. Seifalian, M. Gholipourmalekabadi, *Small* **2021** , 17 , 2006335.
- [28] A. Schulz, K. Januschowski, P. Szurman, *Curr. Opin. Ophthalmol.* **2021** , 32 , 288.
- [29] I. Y. Jung, J. S. Kim, B. R. Choi, K. Lee, H. Lee, *Adv. Healthc. Mater.* **2017** , 6 , 1601475.
- [30] G. C. Le Goff, R. L. Srinivas, W. A. Hill, P. S. Doyle, *Eur. Polym. J.* **2015** , 72 , 386.
- [31] J. Liao, C. Ye, P. Agrawal, Z. Gu, Y. S. Zhang, *Small Structures* **2021** , 2 , 2000110.
- [32] M. I. Lucío, A. Cubells-Gómez, Á. Maquieira, M. Bañuls, *Anal. Bioanal. Chem.* **2022** , 414 , 993.
- [33] C. F. Guimarães, R. Ahmed, A. P. Marques, R. L. Reis, U. Demirci, *Adv. Mater.* **2021** , 33 , 2006582.
- [34] L. Lu, J. D. Joannopoulos, M. Soljačić, *Nat. Photonics* **2014** , 8 , 821.
- [35] A. K. Yetisen, H. Butt, L. R. Volpatti, I. Pavlichenko, M. Humar, S. J. J. Kwok, H. Koo, K. S. Kim, I. Naydenova, A. Khademhosseini, S. K. Hahn, S. H. Yun, *Biotechnol. Adv.* **2016** , 34 , 250.
- [36] Y. Zhao, X. Zhao, Z. Gu, *Adv. Funct. Mater.* **2010** , 20 , 2970.
- [37] M. Umar, K. Min, S. Kim, *APL Photonics* **2019** , 4 , 120901.
- [38] W. Wang, X. Fan, F. Li, J. Qiu, M. M. Umair, W. Ren, B. Ju, S. Zhang, B. Tang, *Adv. Opt. Mater.* **2018** , 6 , 1701093.
- [39] Z. Cai, N. L. Smith, J. Zhang, S. A. Asher, *Anal. Chem.* **2015** , 87 , 5013.
- [40] X. Du, J. Zhai, X. Li, Y. Zhang, N. Li, X. Xie, *ACS Sensors* **2021** , 6 , 1990.
- [41] H. Hu, Q. Chen, K. Cheng, J. Tang, *J. Mater. Chem.* **2012** , 22 , 1021.
- [42] Z. Wang, M. Xue, H. Zhang, Z. Meng, K. J. Shea, L. Qiu, T. Ji, T. Xie, *Rsc Adv.* **2018** , 8 , 9963.
- [43] Y. Sun, Y. Zhang, J. Liu, F. Nie, *Rsc Adv.* **2016** , 6 , 11204.
- [44] H. Zheng, J. Li, W. Song, G. He, Y. Wang, Y. Chen, *Journal of Wuhan University of Technology. Materials science edition* **2021** , 36 , 289.
- [45] M. Lei, Y. Zhang, B. Han, Q. Zhao, A. Zhang, D. Fu, *Ieee Sens. J.* **2018** , 18 , 7499.
- [46] M. Umar, D. Son, S. Arif, M. Kim, S. Kim, *Acs Appl. Mater. Inter.* **2020** , 12 , 55231.
- [47] W. Luo, Q. Cui, K. Fang, K. Chen, H. Ma, J. Guan, *Nano Lett.* **2020** , 20 , 803.
- [48] G. Xie, S. Du, Q. Huang, M. Mo, Y. Gao, M. Li, J. Tao, L. Zhang, J. Zhu, *Acs Appl. Mater. Inter.* **2022** , 14 , 5856.

- [49] Y. Gao, Y. Chen, M. Li, L. Jia, L. Zhang, J. Zhu, *Sensors and Actuators B: Chemical* **2021** , 329 , 129137.
- [50] S. K. Mishra, B. D. Gupta, *Anal. Methods-Uk***2014** , 6 , 5191.
- [51] P. V. N. Kishore, M. Sai Shankar, M. Satyanarayana, *Sensors and Actuators B: Chemical* **2017** , 243 , 626.
- [52] Z. Q. Tou, T. W. Koh, C. C. Chan, *Sensors and Actuators B: Chemical* **2014** , 202 , 185.
- [53] I. M. Savić-Gajić, I. M. Savić, *Expert Opin. Drug Dis.***2020** , 15 , 383.
- [54] T. Chen, Z. Deng, S. Yin, S. Chen, C. Xu, *Journal of materials chemistry. C, Materials for optical and electronic devices***2016** , 4 , 1144.
- [55] F. Lin, L. Yu, *Anal. Methods-Uk* **2012** , 4 , 2838.
- [56] J. Qin, B. Dong, X. Li, J. Han, R. Gao, G. Su, L. Cao, W. Wang, *J. Mater. Chem. C* **2017** , 5 , 8482.
- [57] H. Peng, W. Wang, F. Gao, S. Lin, L. Liu, X. Pu, Z. Liu, X. Ju, R. Xie, L. Chu, *Journal of materials chemistry. C, Materials for optical and electronic devices* **2018** , 6 , 11356.
- [58] X. Wang, G. Ye, X. Wang, *Sensors and Actuators B: Chemical* **2014** , 193 , 413.
- [59] J. Qin, B. Dong, L. Cao, W. Wang, *J. Mater. Chem. C***2018** , 6 , 4234.
- [60] J. H. Holtz, S. A. Asher, *Nature* **1997** , 389 , 829.
- [61] X. Jia, T. Zhang, J. Wang, K. Wang, H. Tan, Y. Hu, L. Zhang, J. Zhu, *Langmuir* **2018** , 34 , 3987.
- [62] W. Hong, Y. Chen, X. Feng, Y. Yan, X. Hu, B. Zhao, F. Zhang, D. Zhang, Z. Xu, Y. Lai, *Chem. Commun.* **2013** , 49 , 8229.
- [63] C. Wang, F. Xiao, Q. Chen, S. Wang, J. Zhou, Z. Wu, *Analyst (London)* **2021** , 146 , 52.
- [64] C. Yan, F. Qi, S. Li, J. Xu, C. Liu, Z. Meng, L. Qiu, M. Xue, W. Lu, Z. Yan, *Talanta* **2016** , 159 , 412.
- [65] B. Maeng, Y. Park, J. Park, *Rsc Adv.* **2016** , 6 , 7384.
- [66] N. Massad-Ivanir, G. Shtenberg, T. Zeidman, E. Segal, *Adv. Funct. Mater.* **2010** , 20 , 2269.
- [67] Z. Cai, D. H. Kwak, D. Punihaole, Z. Hong, S. S. Velankar, X. Liu, S. A. Asher, *Angewandte Chemie* **2015** , 127 , 13228.
- [68] G. Murtaza, A. S. Rizvi, M. Irfan, D. Yan, R. U. Khan, B. Rafique, M. Xue, Z. H. Meng, F. Qu, *Anal. Chim. Acta***2020** , 1117 , 1.
- [69] M. Liu, L. Yu, *The Analyst* **2013** , 138 , 3376.
- [70] R. Zhang, Y. Wang, L. Yu, *J. Hazard. Mater.***2014** , 280 , 46.
- [71] Y. S. Zhang, C. Zhu, Y. Xia, *Adv. Mater.* **2017** , 29 , 1701115.
- [72] X. Zhang, Z. Dai, X. Zhang, S. Dong, W. Wu, S. Yang, X. Xiao, C. Jiang, *Science China Physics, Mechanics & Astronomy***2016** , 59 .
- [73] L. Chen, S. Xu, J. Li, *Chem. Soc. Rev.* **2011** , 40 , 2922.
- [74] G. Sennakesavan, M. Mostakhdemin, L. K. Dkhar, A. Seyfoddin, S. J. Fatihhi, *Polym. Degrad. Stabil.* **2020** , 180 , 109308.
- [75] M. Guo, X. Yu, J. Zhao, J. Wang, R. Qing, J. Liu, X. Wu, L. Zhu, S. Chen, *Sensors and Actuators B: Chemical* **2021** , 347 , 130639.

- [76] R. Liu, Z. Cai, Q. Zhang, H. Yuan, G. Zhang, D. Yang, *Sensors and Actuators B: Chemical* **2022** , 354 , 131236.
- [77] Y. Zhang, Y. Sun, J. Liu, P. Guo, Z. Cai, J. Wang, *Sensors and Actuators B: Chemical* **2019** , 291 , 67.
- [78] J. Yang, Z. Zhu, J. Feng, M. Xue, Z. Meng, L. Qiu, N. Mondele Mbola, *Microchem. J.* **2020** , 157 , 105074.
- [79] W. Liu, L. Li, S. Liu, B. Liu, Z. Wu, J. Deng, *Journal of materials chemistry. C, Materials for optical and electronic devices* **2019** , 7 , 8946.
- [80] N. Zhang, N. Zhang, Y. Xu, Z. Li, C. Yan, K. Mei, M. Ding, S. Ding, P. Guan, L. Qian, C. Du, X. Hu, *Macromol. Rapid Comm.* **2019** , 40 , 1900096.
- [81] J. E. Lofgreen, G. A. Ozin, *Chem. Soc. Rev.* **2014** , 43 , 911.
- [82] Y. Liu, X. Ju, X. Zhou, X. Mu, X. Tian, L. Zhang, Z. Liu, W. Wang, R. Xie, L. Chu, *J. Hazard. Mater.* **2022** , 421 , 126801.
- [83] Y. Yan, M. Yin, W. Hong, Z. Xu, X. Hu, *Rsc Adv.* **2015** , 5 , 97604.
- [84] S. Han, Y. Jin, L. Su, H. Chu, W. Zhang, *Anal. Methods-Uk* **2020** , 12 , 1374.
- [85] J. Hou, H. Zhang, Q. Yang, M. Li, L. Jiang, Y. Song, *Small* **2015** , 11 , 2738.
- [86] X. Wang, Z. Mu, R. Liu, Y. Pu, L. Yin, *Food Chem.* **2013** , 141 , 3947.
- [87] Y. Wang, J. Fan, Z. Meng, M. Xue, L. Qiu, *Anal. Methods-Uk* **2019** , 11 , 2875.
- [88] Y. Li, D. J. Young, X. J. Loh, *Materials Chemistry Frontiers* **2019** , 3 , 1489.
- [89] J. Wu, W. Liu, J. Ge, H. Zhang, P. Wang, *Chem. Soc. Rev.* **2011** , 40 , 3483.
- [90] G. Su, Z. Li, R. Dai, *ACS Applied Polymer Materials* **2022** .
- [91] W. Lu, S. Wei, H. Shi, X. Le, G. Yin, T. Chen, *Aggregate* **2021** , 2 .
- [92] L. M. Wysocki, L. D. Lavis, *Curr. Opin. Chem. Biol.* **2011** , 15 , 752.
- [93] P. P. Jia, S. T. Jiang, L. Xu, *Curr. Org. Synth.* **2019** , 16 , 485.
- [94] M. Natali, S. Campagna, F. Scandola, *Chem. Soc. Rev.* **2010** , 4 , 15.
- [95] R. Martínez-Mañez, F. Sancenón, *Chem. Rev.* **2003** , 103 , 4419.
- [96] J. E. Kwon, S. Y. Park, *Advanced materials (Weinheim)* **2011** , 23 , 3615.
- [97] H. Zong, X. Wang, X. Mu, J. Wang, M. Sun, *The Chemical Record* **2018** , 19 , 818.
- [98] K. Takaishi, K. Iwachido, T. Ema, *J. Am. Chem. Soc.* **2020** , 142 , 1774.
- [99] Y. Zheng, Q. Li, C. Wang, M. Su, *ACS Omega* **2021** , 6 , 11897.
- [100] K. M. Lee, Y. Oh, J. Y. Chang, H. Kim, *J. Mater. Chem. B* **2018** , 6 , 1244.
- [101] K. Zhu, R. Fan, J. Zhang, X. Jiang, W. Jia, B. Wang, H. Lu, J. Wu, P. Wang, Y. Yang, *Dalton T.* **2021** , 50 , 15679.
- [102] J. Bartelmess, V. Valderrey, K. Rurack, *Frontiers in Chemistry* **2019** , 7 .
- [103] S. Xiong, W. Sun, R. Chen, Z. Yuan, X. Cheng, *Carbohydr. Polym.* **2021** , 273 , 118590.
- [104] R. Gotor, P. Ashokkumar, M. Hecht, K. Keil, K. Rurack, *Anal. Chem.* **2017** , 89 , 8437.
- [105] S. Radunz, E. Andresen, C. Würth, A. Koerd, H. R. Tschiche, U. Resch-Genger, *Anal. Chem.* **2019** , 91 , 7756.

- [106] M. Maierhofer, V. Rieger, T. Mayr, *Anal. Bioanal. Chem.* **2020** , 412 , 7559.
- [107] H. D. Duong, R. Jong Il, *Sensors and Actuators B: Chemical* **2018** , 274 , 66.
- [108] L. Xiong, J. Feng, R. Hu, S. Wang, S. Li, Y. Li, G. Yang, *Anal. Chem.* **2013** , 85 , 4113.
- [109] N. Parshi, D. Pan, B. Jana, J. Ganguly, *Sensors and Actuators B: Chemical* **2021** , 331 , 129419.
- [110] D. Biswakarma, N. Dey, S. Bhattacharya, *Chem. Sci.* **2022** , 13 , 2286.
- [111] Rohini, K. Paul, V. Luxami, *Chem. Rec.* **2020** , 20 , 1430.
- [112] Y. Yue, J. Gu, J. Han, Q. Wu, J. Jiang, *J. Hazard. Mater.* **2021** , 401 , 123798.
- [113] Z. Song, F. Wang, J. Qiang, Z. Zhang, Y. Chen, Y. Wang, W. Zhang, X. Chen, *J. Lumin.* **2017** , 183 , 212.
- [114] N. Dave, M. Y. Chan, P. J. Huang, B. D. Smith, J. Liu, *J. Am. Chem. Soc.* **2010** , 132 , 12668.
- [115] X. Mao, D. Mao, J. Jiang, B. Su, G. Chen, X. Zhu, *Lab Chip* **2021** , 21 , 154.
- [116] K. Pi, J. Liu, P. Van Cappellen, *J. Hazard. Mater.* **2020** , 385 , 121572.
- [117] L. Zhang, Q. Cai, J. Li, J. Ge, J. Wang, Z. Dong, Z. Li, *Biosensors and Bioelectronics* **2015** , 69 , 77.
- [118] Z. Qing, Z. Mao, T. Qing, X. He, Z. Zou, D. He, H. Shi, J. Huang, J. Liu, K. Wang, *Anal. Chem.* **2014** , 86 , 11263.
- [119] J. Chen, T. Han, X. Feng, B. Wang, G. Wang, *Analyst* **2019** , 144 , 2423.
- [120] X. Yan, H. Li, T. Hu, X. Su, *Biosensors and Bioelectronics* **2017** , 91 , 232.
- [121] J. Peng, J. Ling, Q. Wen, Y. Li, Q. Cao, Z. Huang, Z. Ding, *Rsc Adv.* **2018** , 8 , 41464.
- [122] A. Aliberti, A. M. Cusano, E. Battista, F. Causa, P. A. Netti, *Analyst (London)* **2016** , 141 , 1250.
- [123] L. Xu, R. Wang, L. C. Kelso, Y. Ying, Y. Li, *Sensors and Actuators B: Chemical* **2016** , 234 , 98.
- [124] T. V. Dao, K. Herbst, K. Boerner, M. Meurer, L. P. Kremer, D. Kirrmaier, A. Freistaedter, D. Pappagiannidis, C. Galmozzi, M. L. Stanifer, S. Boulant, S. Klein, P. Chlanda, D. Khalid, M. I. Barreto, P. Schnitzler, H. G. Krausslich, M. Knop, S. Anders, *Sci. Transl. Med.* **2020** , 12 .
- [125] Y. Zhu, X. Wu, A. Gu, L. Dobbelle, C. A. Cid, J. Li, M. R. Hoffmann, *Environ. Sci. Technol.* **2022** , 56 , 862.
- [126] B. A. Baker, V. T. Milam, *Nucleic Acids Res.* **2011** , 39 , e99.
- [127] D. C. Pregibon, P. S. Doyle, *Anal. Chem.* **2009** , 81 , 4873.
- [128] A. Beyer, S. Pollok, A. Rudloff, D. Cialla-May, K. Weber, J. Popp, *Macromol. Biosci.* **2016** , 16 , 1325.
- [129] L. Hao, W. Wang, X. Shen, S. Wang, Q. Li, F. An, S. Wu, *J. Agr. Food Chem.* **2020** , 68 , 369.
- [130] M. Kim, J. E. Kwon, K. Lee, W. G. Koh, *Biofabrication* **2018** , 10 , 35002.
- [131] D. Su, X. Zhao, X. Yan, X. Han, Z. Zhu, C. Wang, X. Jia, F. Liu, P. Sun, X. Liu, G. Lu, *Biosensors and Bioelectronics* **2021** , 194 , 113598.
- [132] R. Jin, D. Kong, X. Yan, X. Zhao, H. Li, F. Liu, P. Sun, Y. Lin, G. Lu, *Acs Appl. Mater. Inter.* **2019** , 11 , 27605.
- [133] C. Sahub, J. L. Andrews, J. P. Smith, M. A. Mohamad Arif, B. Tomapatanaget, J. W. Steed, *Materials Chemistry Frontiers* **2021** , 5 , 6850.
- [134] S. Huang, J. Yao, B. Li, G. Ning, Q. Xiao, *Mikrochimica acta (1966)* **2021** , 188 , 318.

- [135] E. Jang, K. J. Son, B. Kim, W. Koh, *The Analyst***2010** , 135 , 2871.
- [136] S. Park, E. Jang, W. Koh, B. Kim, *Talanta***2011** , 84 , 1000.
- [137] S. Park, E. Jang, W. Koh, B. Kim, *Sensors and Actuators B: Chemical* **2010** , 150 , 120.
- [138] J. Wang, J. Zhang, J. Wang, G. Fang, J. Liu, S. Wang, *J. Hazard. Mater.* **2020** , 389 , 122074.
- [139] Z. Díaz-Betancor, M. Bañuls, F. J. Sanza, R. Casquel, M. F. Laguna, M. Holgado, R. Puchades, Á. Maquieira, *Microchim. Acta***2019** , 186 .
- [140] A. M. L. Piloto, D. S. M. Ribeiro, S. S. M. Rodrigues, J. L. M. Santos, P. Sampaio, M. G. F. Sales, *Microchim. Acta***2022** , 189 .
- [141] J. Yan, Y. Sun, H. Zhu, L. Marcu, A. Revzin, *Biosensors and Bioelectronics* **2009** , 24 , 2604.
- [142] E. Petryayeva, W. R. Algar, I. L. Medintz, *Appl. Spectrosc.* **2013** , 67 , 215.
- [143] C. Matea, T. Mocan, F. Tabaran, T. Pop, O. Mosteanu, C. Puia, C. Iancu, L. Mocan, *International Journal of Nanomedicine***2017** , Volume 12 , 5421.
- [144] K. D. Wegner, N. Hildebrandt, *Chem. Soc. Rev.***2015** , 44 , 4792.
- [145] S. N. Baker, G. A. Baker, *Angewandte Chemie International Edition* **2010** , 49 , 6726.
- [146] F. Yuan, S. Li, Z. Fan, X. Meng, L. Fan, S. Yang, *Nano Today* **2016** , 11 , 565.
- [147] M. Batool, H. M. Junaid, S. Tabassum, F. Kanwal, K. Abid, Z. Fatima, A. T. Shah, *Crit. Rev. Anal. Chem.* **2020** , 1.
- [148] X. Chen, Z. Song, B. Yuan, X. Li, S. Li, T. Thang Nguyen, M. Guo, Z. Guo, *Chem. Eng. J.* **2022** , 430 , 133154.
- [149] C. Cheng, M. Xing, Q. Wu, *J. Alloy. Compd.***2019** , 790 , 221.
- [150] F. Cheng, S. Zhang, L. Zhang, J. Sun, Y. Wu, *Colloids and Surfaces A: Physicochemical and Engineering Aspects* **2022** ,636 , 128149.
- [151] X. Guo, D. Xu, H. Yuan, Q. Luo, S. Tang, L. Liu, Y. Wu, *Journal of materials chemistry. A, Materials for energy and sustainability* **2019** , 7 , 2781.
- [152] H. Huang, H. Ge, Z. Ren, Z. Huang, M. Xu, X. Wang, *Frontiers in Bioengineering and Biotechnology* **2021** ,9 .
- [153] Q. Luo, H. Yuan, M. Zhang, P. Jiang, M. Liu, D. Xu, X. Guo, Y. Wu, *J. Hazard. Mater.* **2021** , 401 , 123432.
- [154] H. Yuan, J. Peng, T. Ren, Q. Luo, Y. Luo, N. Zhang, Y. Huang, X. Guo, Y. Wu, *Sci. Total Environ.* **2021** , 760 , 143395.
- [155] Y. Chen, L. Zhang, Y. Yang, B. Pang, W. Xu, G. Duan, S. Jiang, K. Zhang, *Advanced materials (Weinheim)* **2021** , 33 , e2005569.
- [156] Y. H. Jung, T. Chang, H. Zhang, C. Yao, Q. Zheng, V. W. Yang, H. Mi, M. Kim, S. J. Cho, D. Park, H. Jiang, J. Lee, Y. Qiu, W. Zhou, Z. Cai, S. Gong, Z. Ma, *Nat. Commun.* **2015** , 6 .
- [157] D. Zhang, X. Tian, H. Li, Y. Zhao, L. Chen, *Colloids and Surfaces A: Physicochemical and Engineering Aspects* **2021** ,608 , 125563.
- [158] J. Xu, X. Jie, F. Xie, H. Yang, W. Wei, Z. Xia, *Nano Res.* **2018** , 11 , 3648.
- [159] L. Sun, Z. Mo, Q. Li, D. Zheng, X. Qiu, X. Pan, *Int. J. Biol. Macromol.* **2021** , 175 , 516.
- [160] Z. Jiao, J. Li, L. Mo, J. Liang, H. Fan, *Mikrochim Acta***2018** , 185 , 473.

- [161] S. Zhang, K. Arkin, Y. Zheng, J. Ma, Y. Bei, D. Liu, Q. Shang, *Journal of environmental chemical engineering* **2022** , *10* , 106921.
- [162] J. Yang, X. Jin, Z. Cheng, H. Zhou, L. Gao, D. Jiang, X. Jie, Y. Ma, W. Chen, *Acs Sustain. Chem. Eng.* **2021** , *9* , 13206.
- [163] X. Yang, Y. Yang, M. Xu, S. Liang, X. Pu, J. Hu, Q. Li, J. Zhao, Z. Zhang, *ACS applied nano materials* **2021** , *4* , 13986.
- [164] X. Yan, S. Rahman, M. Rostami, Z. A. Tabasi, F. Khan, A. Alodhayb, Y. Zhang, *ACS Omega* **2021** , *6* , 23504.
- [165] H. Ehtesabi, S. Roshani, Z. Bagheri, M. Yaghoubi-Avini, *Journal of Environmental Chemical Engineering* **2019** , *7* , 103419.
- [166] Y. Li, Y. Wang, P. Du, L. Zhang, Y. Liu, X. Lu, *Sensors and Actuators B: Chemical* **2022** , *358* , 131526.
- [167] Y. Hu, R. Guan, S. Zhang, X. Fan, W. Liu, K. Zhang, X. Shao, X. Li, Q. Yue, *Food Chem.* **2022** , *372* , 131287.
- [168] Y. Li, C. Mou, Z. Xie, M. Zheng, *Dyes Pigments* **2022** , *198* , 110023.
- [169] S. Bhattacharya, S. Nandi, R. Jelinek, *Rsc Adv.* **2017** , *7* , 588.
- [170] Y. Cai, M. Wang, M. Liu, J. Zhang, Y. Zhao, *Advanced materials interfaces* **2022** , *9* , 2101633.
- [171] L. Sun, Z. Mo, Q. Li, D. Zheng, X. Qiu, X. Pan, *Int. J. Biol. Macromol.* **2021** , *175* , 516.
- [172] S. Iravani, R. S. Varma, *Environ. Chem. Lett.* **2020** , *18* , 703.
- [173] X. T. Zheng, A. Ananthanarayanan, K. Q. Luo, P. Chen, *Small* **2015** , *11* , 1620.
- [174] Y. Yan, J. Gong, J. Chen, Z. Zeng, W. Huang, K. Pu, J. Liu, P. Chen, *Advanced materials (Weinheim)* **2019** , *31* , e1808283.
- [175] L. Lin, M. Rong, F. Luo, D. Chen, Y. Wang, X. Chen, *TrAC Trends in Analytical Chemistry* **2014** , *54* , 83.
- [176] S. Chung, R. A. Revia, M. Zhang, *Advanced materials (Weinheim)* **2021** , *33* , e1904362.
- [177] J. Ding, X. Zhou, Y. Huang, B. Chen, S. Chen, Y. Jin, Y. Yang, N. Pan, C. Xu, J. Chen, C. Xia, *Appl. Surf. Sci.* **2022** , *583* , 152492.
- [178] S. Lai, Y. Jin, L. Shi, Y. Li, R. Zhou, *Chem. Eng. J.* **2022** , *429* , 132367.
- [179] L. Nana, L. Ruiyi, G. Wang, Z. Haiyan, Z. Li, *New J. Chem.* **2022** , *46* , 9408.
- [180] D. Jiang, M. Qin, L. Zhang, X. Shan, Z. Chen, *Sensors and Actuators B: Chemical* **2021** , *345* , 130343.
- [181] R. Hua, N. Hao, J. Lu, J. Qian, Q. Liu, H. Li, K. Wang, *Biosensors and Bioelectronics* **2018** , *106* , 57.
- [182] X. Pham, S. Park, K. Ham, S. Kyeong, B. S. Son, J. Kim, E. Hahm, Y. Kim, S. Bock, W. Kim, S. Jung, S. Oh, S. H. Lee, D. W. Hwang, B. Jun, *Int. J. Mol. Sci.* **2021** , *22* , 10116.
- [183] E. Bagheri, L. Ansari, K. Abnous, S. M. Taghdisi, P. Ramezani, M. Ramezani, M. Alibolandi, *Crit. Rev. Anal. Chem.* **2021** , *51* , 687.
- [184] J. Chen, Y. Yu, B. Zhu, J. Han, C. Liu, C. Liu, L. Miao, S. Fakudze, *Sci. Total Environ.* **2021** , *765* , 142754.
- [185] J. Wang, X. Ma, L. Wei, G. Dai, X. Zhu, Y. Zhu, T. Mei, J. Li, X. Wang, *Mater. Express* **2017** , *7* , 351.

- [186] R. Li, L. Li, B. Wang, L. Yu, *Nanomaterials***2021** , 11 , 3126.
- [187] H. Ren, Y. Fan, B. Wang, L. Yu, *J. Agr. Food Chem.***2018** , 66 , 8851.
- [188] N. Qi, H. Zhao, Q. Wang, Y. Qin, H. Yuan, Y. Li, *Soft Matter* **2019** , 15 , 2319.
- [189] T. Hu, J. Xu, Y. Ye, Y. Han, X. Li, Z. Wang, D. Sun, Y. Zhou, Z. Ni, *Biosensors and Bioelectronics* **2019** , 136 , 112.
- [190] A. S. Hoffman, *Adv. Drug Deliver. Rev.* **2012** ,64 , 18.
- [191] T. Jang, H. Jung, H. M. Pan, W. T. Han, S. Chen, J. Song,*International Journal of Bioprinting* **2018** , 4 .
- [192] S. Utech, A. R. Boccaccini, *J. Mater. Sci.***2016** , 51 , 271.
- [193] M. Abbas, M. Adil, S. Ehtisham-Ul-Haque, B. Munir, M. Yameen, A. Ghaffar, G. A. Shar, M. Asif Tahir, M. Iqbal, *Sci. Total Environ.* **2018** , 626 , 1295.
- [194] X. Nie, J. Zhang, X. Jiang, S. Liu, H. Cui, P. Yang, G. Sui,*Anal. Methods-Uk* **2013** , 5 , 4386.
- [195] R. Ranjan, N. K. Rastogi, M. S. Thakur, *J. Hazard. Mater.* **2012** , 225-226 , 114.
- [196] K. Y. Lee, D. J. Mooney, *Prog. Polym. Sci.***2012** , 37 , 106.
- [197] S. N. Pawar, K. J. Edgar, *Biomaterials* **2012** ,33 , 3279.
- [198] N. Gou, A. Z. Gu, *Environ. Sci. Technol.* **2011** ,45 , 5410.
- [199] N. Gou, A. Onnis-Hayden, A. Z. Gu, *Environ. Sci. Technol.* **2010** , 44 , 5964.
- [200] J. Lan, N. Gou, S. M. Rahman, C. Gao, M. He, A. Z. Gu,*Environ. Sci. Technol.* **2016** , 50 , 3202.
- [201] J. Lan, M. Hu, C. Gao, A. Alshwabkeh, A. Z. Gu,*Environ. Sci. Technol.* **2015** , 49 , 6284.
- [202] A. Zaslaver, A. Bren, M. Ronen, S. Itzkovitz, I. Kikoin, S. Shavit, W. Liebermeister, M. G. Surette, U. Alon, *Nat. Methods***2006** , 3 , 623.
- [203] A. Zaslaver, S. Kaplan, A. Bren, A. Jinich, A. Mayo, E. Dekel, U. Alon, S. Itzkovitz, *PLoS Comput Biol* **2009** , 5 , e1000545.
- [204] L. Torres, A. Krüger, E. Csibra, E. Gianni, V. B. Pinheiro,*Essays Biochem.* **2016** , 60 , 393.
- [205] G. V. Dana, T. Kuiken, D. Rejeski, A. A. Snow, *Nature***2012** , 483 , 29.
- [206] B. Shemer, E. Shpigel, C. Hazan, Y. Kabessa, A. J. Agranat, S. Belkin, *Microbial Biotechnology* **2021** , 14 , 251.
- [207] E. Elcin, F. Ayaydin, H. A. ökten, *Int. J. Environ. An. Ch.* **2021** , 1.
- [208] E. Eltzov, A. Cohen, R. S. Marks, *Anal. Chem.***2015** , 87 , 3655.
- [209] V. Fleischauer, J. Heo, *Anal. Sci.* **2014** ,30 , 937.
- [210] T. Elad, R. Almog, S. Yagur-Kroll, K. Levkov, S. Melamed, Y. Shacham-Diamand, S. Belkin, *Environ. Sci. Technol.* **2011** ,45 , 8536.
- [211] S. Jouanneau, M. J. Durand, G. Thouand, *Environ. Sci. Technol.* **2012** , 46 , 11979.
- [212] N. ~uržul, B. T. Stokke, *Biosensors* **2021** ,11 , 266.
- [213] M. Elsherif, M. U. Hassan, A. K. Yetisen, H. Butt, *Biosensors and Bioelectronics* **2019** , 137 , 25.
- [214] J. Guo, B. Zhou, Z. Du, C. Yang, L. Kong, L. Xu, *Nanophotonics***2021** , 10 , 3549.
- [215] J. Li, J. Zhang, H. Sun, D. Hong, L. Li, Y. Yang, X. Yong, C. Zhang, J. Cui,*Optik* **2019** , 195 , 163172.

- [216] A. Francone, T. Kehoe, I. Obieta, V. Saez-Martinez, L. Bilbao, A. Khokhar, N. Gadegaard, C. Simao, N. Kehagias, C. Sotomayor Torres, *Sensors-Basel* **2018** , 18 , 3240.
- [217] S. R. Makhsin, N. J. Goddard, R. Gupta, P. Gardner, P. J. Scully, *Anal. Chem.* **2020** , 92 , 14907.
- [218] Q. Zhang, Y. Wang, A. Mateescu, K. Sergelen, A. Kibrom, U. Jonas, T. Wei, J. Dostalek, *Talanta* **2013** , 104 , 149.
- [219] Y. Alqurashi, M. Elsherif, A. Hendi, K. Essa, H. Butt, *Biosensors* **2022** , 12 , 40.
- [220] S. Chen, H. Sun, Z. Huang, Z. Jin, S. Fang, J. He, Y. Liu, Y. Zhang, J. Lai, *Rsc Adv.* **2019** , 9 , 16831.
- [221] S. Jung, K. I. Macconaghy, M. T. Guarnieri, J. L. Kaar, M. P. Stoykovich, *ACS Applied Bio Materials* **2022** , 5 , 1252.
- [222] X. Bao, J. Liu, Q. Zheng, W. Pei, Y. Yang, Y. Dai, T. Tu, *Chinese Chem. Lett.* **2019** , 30 , 2266.
- [223] J. An, Y. Shi, J. Fang, Y. Hu, Y. Liu, *Chem. Eng. J.* **2021** , 425 , 130595.
- [224] X. Dai, Y. Deng, X. Peng, Y. Jin, *Adv. Mater.* **2017** , 29 , 1607022.
- [225] Y. Shirasaki, G. J. Supran, M. G. Bawendi, V. Bulovic, *Nat. Photonics* **2013** , 7 , 13.
- [226] C. Dalwadi, G. Patel, *Recent Pat. Nanotech.* **2015** , 9 , 17.
- [227] G. Granata, S. Petralia, G. Forte, S. Conoci, G. M. L. Consoli, *Materials Science and Engineering: C* **2020** , 111 , 110842.